

PART III:

FGS

Chapter 9: FGS Instrument Overview

Chapter 10: FGS Data Structures

Chapter 11: FGS Calibration

Chapter 12: FGS Error Sources

Chapter 13: FGS Data Analysis

■ FGS

FGS Overview

In This Chapter...

FGS Capabilities / 9-2
FGS Design / 9-3
FGS Control / 9-15
Target Acquisition and Tracking / 9-16
Transfer Scans / 9-21
FGS Guiding / 9-21
FGS Astrometry / 9-22
Astrometry with FGS 3 / 9-23

The primary purpose of the three Fine Guidance Sensors (FGS) on HST is to maintain the pointing stability of the telescope at the milliarcsecond level. The FGSs, designed and built by Hughes Danbury Optical Systems (HDOS), routinely point the spacecraft with a precision of 5 mas or less. As part of the second servicing mission, HDOS upgraded the spare FGS, which replaced the original in Bay #1, with a commandable mechanism to enhance the instrument's performance. HDOS is currently upgrading the returned FGS1 for an expected return to the telescope during the third servicing mission.

The high precision of the FGSs makes them excellent astrometers. The narrow point spread function of HST and the dynamic range of the FGS make it an unparalleled science instrument for many important astronomical investigations. Detecting and resolving multiple star systems and planetary companions, delineation of objects in crowded fields, measuring stellar angular diameters, parallax, proper motion, positional surveys, occultation studies and photometry are among its many uses. This chapter describes how each Fine Guidance Sensor operates, summarizing its capabilities, its design, and its modes of operation.

9.1 FGS Capabilities

Each Fine Guidance Sensor on HST is an optical-mechanical white-light interferometer that can sense 1–2 milliarcsecond (mas) angular displacements of a point source in two dimensions over the range of apparent visual magnitudes from $3 < V < 15$. It can observe fainter objects down to $V < 17$, but its accuracy degrades to more than 2 mas. The instrument's spectral response is fairly flat from 4000 Å to 7200 Å, although more sensitive in the red, with sharp drop-offs outside this range.

The optical path through an FGS is complex because the beam passes through multiple optical elements. The relative alignment of all these components and the wavelength dependencies introduced by their reflective surfaces and refractive optics impose the resolution and magnitude limits of the FGS. Most of the FGS calibration procedure consists of empirical and semi-empirical subtraction of the instrument's signature, necessitating observations of standard stars in various spectral ranges and all modes of observation.

The three FGSs on board HST occupy three of the four radial bays. Normally two FGSs are used for pitch, yaw, and roll control of the telescope, leaving one available for astrometry. The telemetry from the guiding FGSs is captured and processed by the ground system and stored in the Hubble Data Archive. The processed FGS data can be retrieved for any HST observation in the form of OMS files (see Appendix B), which provide information on spacecraft jitter. However, the data files associated with an FGS astrometry observation, which are used in the FGS calibration pipeline, record jitter information at a much higher time resolution (40 Hz as compared to 0.33 Hz).

An FGS can be used for astrometry in two different modes:

- POSITION mode, in which it tracks an object, measuring its precise location.
- TRANSFER mode, in which it scans across an object, such as a binary star system, resolving its structure.

POSITION mode observing is used both to guide the telescope and for positional astrometry. TRANSFER mode is used primarily to support astrometry science programs investigating multiple star systems or extended objects, but is on occasion used in engineering tests to evaluate the FGS and the OTA optical systems.

FGS 3 is currently designated and calibrated as an astrometer. This FGS can measure point-source angular positions of 1–2 mas over the brightness range of 3 to 17 magnitudes and can resolve the components of binary systems with separations as small as 15 mas. For many scientific studies, this FGS continues to exceed ground based efforts in sensitivity, dynamic range, and resolution.

9.2 FGS Design

This section describes the Fine Guidance Sensor design, its optical train, the aperture, the S-curves that give the response of the instrument to positional changes, and the enhancements made to the refurbished FGS 1R, installed during the February 1997 servicing mission.

9.2.1 FGS Optics

An FGS is essentially a pair of two orthogonal white-light, equal-path interferometers, their associated optical and mechanical elements, and four photo-multiplier tubes (PMTs). Light from an object is collected by the telescope's primary mirror, reflected and focused by the secondary mirror, intercepted by a plane pickoff mirror before the focal point, and directed into the FGS and onto the Aspheric Collimating Mirror to produce a nearly collimated beam. The ray is directed to the optical elements of the Star Selector A (SSA) assembly. This rigid assembly of two mirrors and a five element corrector group can be commanded to rotate about HST's optical axis (V1). Two mirrors in the Star Selector A assembly deflect the beam and direct it through the five element corrector group that performs the final collimation and corrects for the optical aberrations induced by the aspheric mirror. They do not correct the spherical aberration arising from HST's mis-figured primary mirror.

The direction of the exit ray depends upon the incoming beam's angle of incidence on the SSA assembly, and therefore the rotation position of SSA and the beam's point of origin on the aspheric mirror which is, in turn, determined by the angle between the spacecraft's optical axis (V1) and the position of the star on the sky.

After exiting the SSA assembly the ray encounters a field stop to minimize scattered light and to narrow the field of view. The four mirrors of the Star Selector B (SSB) assembly receive the ray and redirect it through the filter wheel assembly and a plane fold flat mirror (FF3) reflects it onto the polarizing beam splitter. Like the SSA assembly, the SSB assembly can be commanded to rotate within HST's focal plane. Together the SSA and SSB assemblies transmit to the polarizing beam splitter only those photons originating from a narrowly defined direction, masking out all but a small (5" x 5") area of sky.

The polarizing beam splitter divides the incoming unpolarized light into two linearly plane polarized beams with orthogonal polarizations, each having roughly half the incident intensity, and directs them to the two Koesters prisms and their associated optics, field stops, and photomultiplier tubes (see Figure 9.1). Each of the two output rays from the polarizing beam splitter fall upon the face of the appropriate Koesters prism.

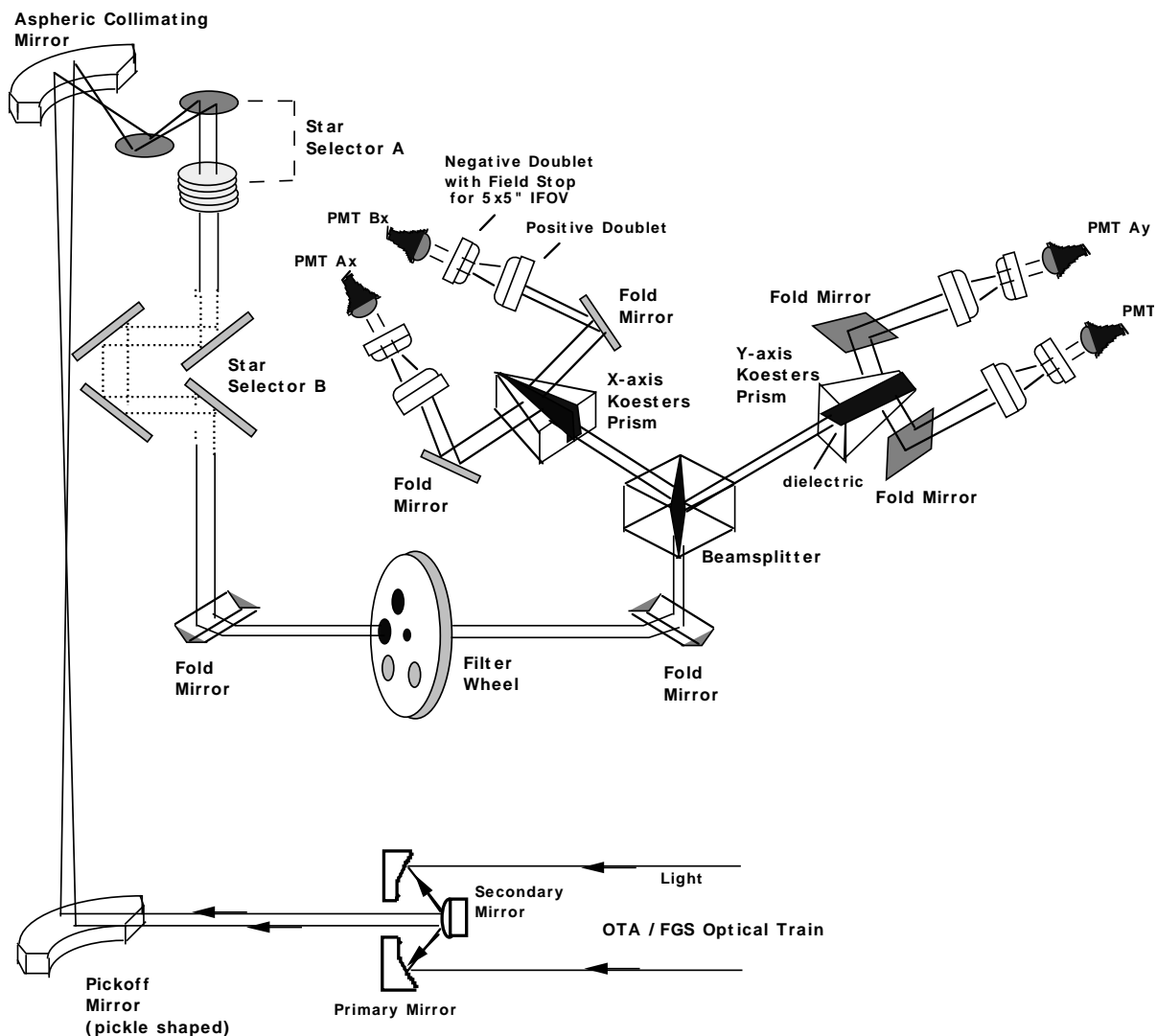
The Koesters prisms are constructed of two halves of fused silica joined together along a surface coated to act as a dielectric beam splitter. The dielectric performs an equal intensity division, introducing a 90 degree phase difference between the reflected and transmitted portions of the beam, with the transmitted

lagging the reflected. This division gives the Koesters prism its interferometric properties because the beam reflected from one side of the prism, when joined with the transmitted beam from the other side, constructively or destructively interferes to a degree depending upon the angle between the incoming wavefront and the entrance face. Each Koesters prism thus emits two collimated exit beams whose relative intensities depend upon the tilt of the incident wavefront. Each beam is then focused and passed through a field stop to illuminate the surface of a photomultiplier tube (PMT) which records the number of photons received during each 25 msec interval.

The collimated beam entering each Koesters prism can be characterized by a propagation vector. The Koesters prism senses the tilt of this incident wavefront only in the direction perpendicular to the plane of the dielectric surface. Small rotations of the star selector A and B assemblies can change the direction of the propagation vector, and hence the tilt of the incident wavefront at the face of the Koesters prism. When the component of the wavefront's propagation vector perpendicular to the plane of the dielectric surface is zero, a condition of interferometric null results, and the relative intensities of the two emergent beams, measured by the PMTs, will ideally be equal. Meanwhile, the other Koesters prism is sensitive to the wavefront's tilt in the orthogonal plane.

Figure 9.1 schematically displays the important optical and mechanical components of an FGS. Each Koesters prism is sensitive to the tilt of the wavefront about an axis which is parallel to the face of the prism and in the plane of the dielectric beam splitter (the shaded area within each prism).

Figure 9.1: The FGS Optical Train



The fine sensitivity of the Koesters prisms to the angle of the incident radiation is what enables the FGS to measure star positions so accurately. For a star at a given position in FGS's detector space, there is a unique rotational position for each of the star selector A,B assemblies which brings that star's wavefront to zero tilt at the face of each Koesters prism. Therefore, the position of the star in the FGS detector space, and equivalently in HST's focal plane, can be measured precisely and accurately. Ultimately, the reliability of such measurements depends on the calibration of the instrument.

An (x,y) coordinate system maps the detector space of an FGS. The Koesters prisms are aligned such that one is sensitive to angular displacements along the x direction, the other along the y direction. Because each Koesters prism has two associated PMTs, each FGS has four PMTs in all. The two PMTs associated with

the x -axis Koesters prism are labeled PMTXA and PMTXB. The other pair, associated with the y -axis Koesters prism, are labeled PMTYA and PMTYB.



Note that the FGS (x,y) detector coordinate system differs from the POS TARG coordinate system in the Phase II proposal instructions. The FGS coordinates originate from the telescope's optical axis (V1 bore sight) while the POS TARG system originates from the center of the detector's field of view. The POS TARG system is used to conveniently define offsets.

9.2.2 FGS Aperture

The instrument's total field of view (FOV), referred to as a *pickle* because it vaguely resembles the shape of a pickle, is a quarter annulus in the HST's focal plane, extending radially 10' to 14' from the telescope's boresight and axially 83.3° on the inner arc and 85° on its outer arc, an area of approximately 69 square arcminutes. The instantaneous field of view (IFOV) determined by the star selector assemblies and field stops is far smaller—5" by 5"—and its location within the pickle depends upon the Star Selector A and B rotation angles. Only those photons entering this IFOV aperture will be registered by the PMTs. To observe stars elsewhere, the star selector assemblies must be rotated to bring the IFOV to the target. This procedure is called *slewing* the IFOV.

The (x,y) location of the IFOV in the total FOV is determined from the rotation angles of the star selector A,B assemblies. Each FGS has its own detector space (x,y) coordinate system which maps into HST's (V1,V2,V3) coordinate system. FGS 2, and FGS 3 are nominally oriented at 90, and 180 degrees with respect to FGS 1, but small angular deviations are present. The FGS-to-FGS alignment matrix in the onboard flight software accounts for these deviations. Figure 9.2 and Figure 9.3 show the FGSs and their coordinate systems in the HST focal plane.

Figure 9.2: FGS Field of View (pickle) the HST Focal Plane with Local (x,y) Coordinate System Related to HST (V2,V3) System.

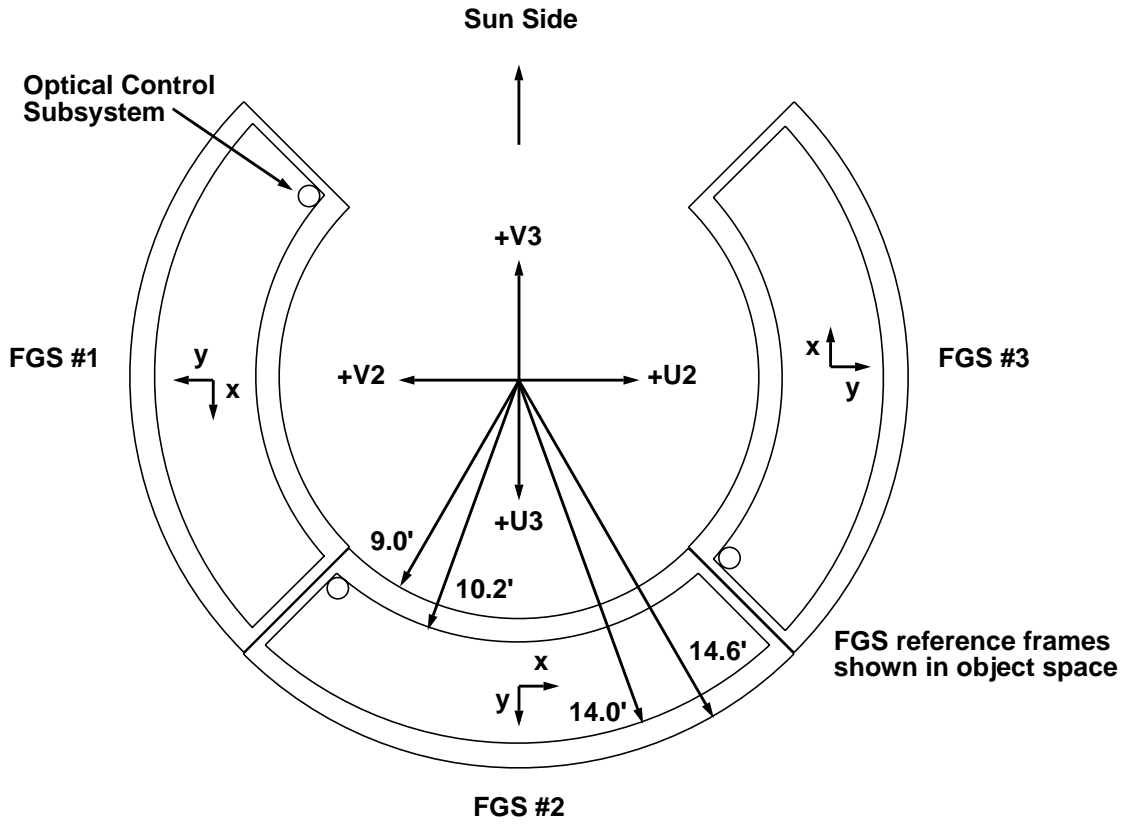
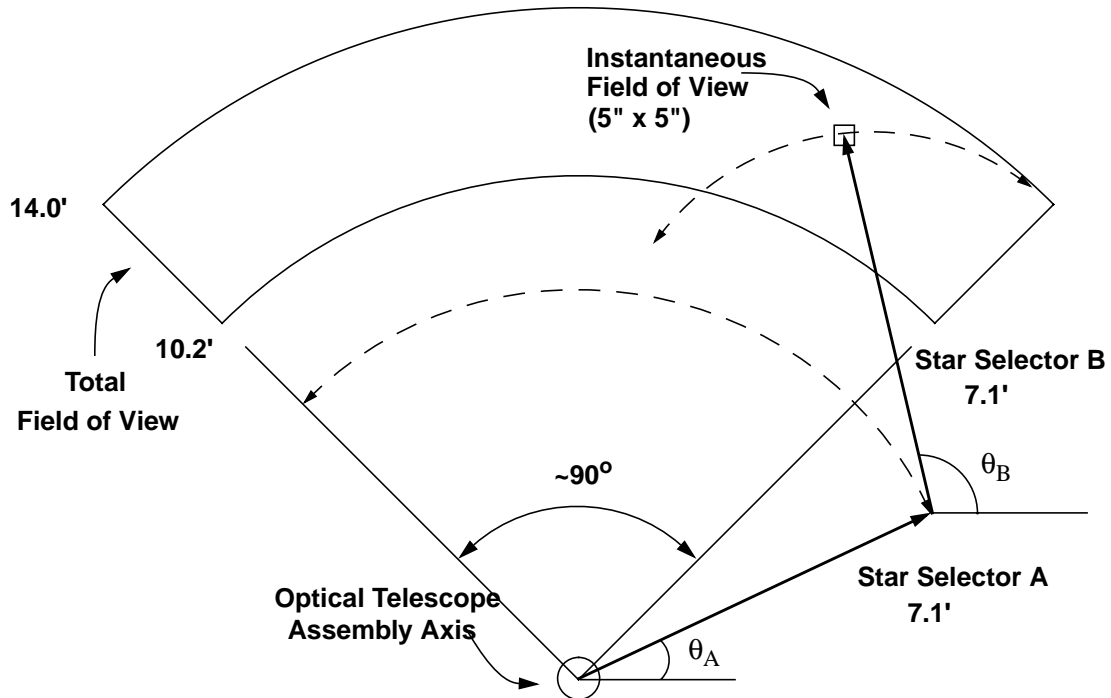
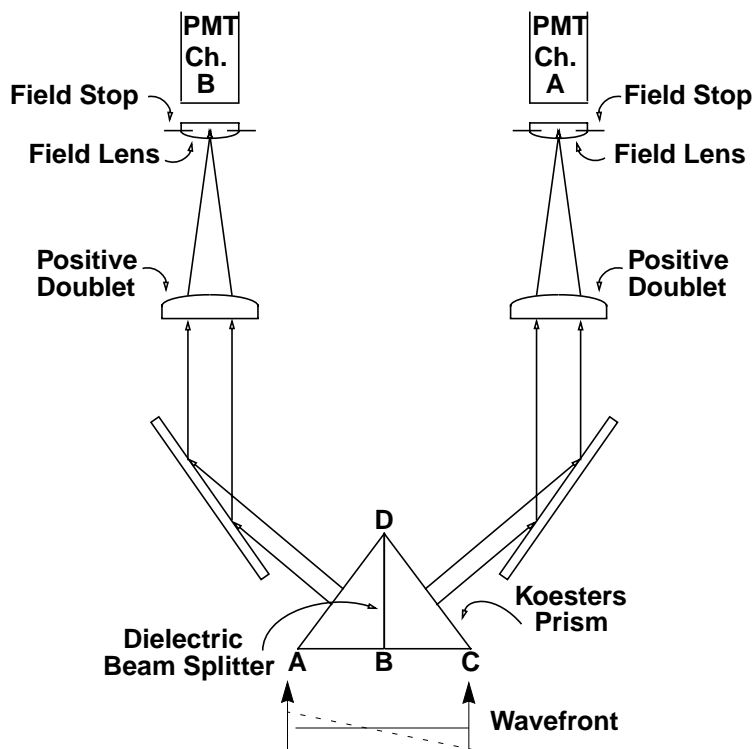


Figure 9.3: IFOV Placement in Pickle by Rotating SSA and SSB.

9.2.3 S-curves

As discussed earlier, each Koesters prism in an FGS is sensitive to the tilt of the incident wavefront in the direction perpendicular to the dielectric surface joining the two halves of the prism (see Figure 9.4, and Figure 9.5). Assuming the presence of a luminous point source in the IFOV, the relative intensity of the beams emerging from each Koesters prism is determined by the wavefront's tilt, and therefore responds to the rotations of the SSA and SSB assemblies that scan the IFOV across the star. The responses of the PMTs during such a scan provide the characteristic interferometric signature of the FGS. Graphing the normalized difference of the PMTs corresponding to a given channel against the position of the IFOV in detector space produces a figure known as an *S-curve*.

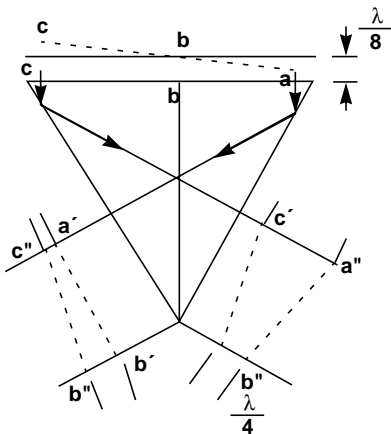
Figure 9.4: Emergent Beams from Koesters Prism and Photo-multiplier Tubes. The Koesters prism is sensitive to the tilt of the wavefront about an axis normal to the page and intersecting point B.



FGS/9

Figure 9.5 shows how a Koesters prism generates the characteristic S-curves shown in Figure 9.6. As the wavefront rotates about point B, the relative intensities of the two emergent beams change as a function of the tilt angle. If the tilt axis is not at point B, the beam is said to be *decentered* and the S-curve's morphology and modulation are degraded. Unfortunately, because HST's wavefront is spherically aberrated, a small decenter of the beam (0.5%) will cause 25% degradation of the S-curve's signal.

Figure 9.5: Internal Reflection and Transmission of the Beam Entering the Koesters Prism on the AC Face

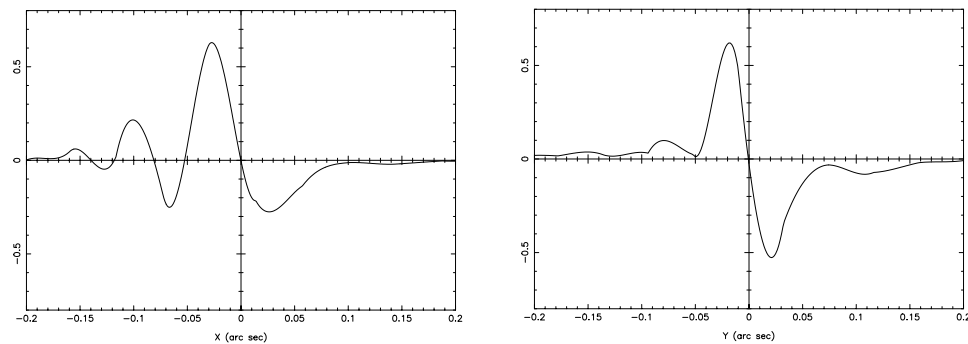


The Koesters prisms measure the two orthogonal wavefront directions and thus produces two S-curves, S_x and S_y . The x -axis S-curve is given by:

$$S_x = (A_x - B_x) / (A_x + B_x)$$

where A_x is the photon count from PMTXA (accumulated over 25msec), and B_x is the count from PMTXB. The y -axis S-curve is computed in a similar way. Figure 9.6 shows the S-curves for the x and y axes observed near the center of the field of view of FGS 3. When the IFOV is more than 100 mas from the location of interferometric null, the PMTs of a given channel record nearly equal intensities. But closer to the interferometric null a signal emerges as the Koesters prism produces beams of different relative intensities. The so-called *zero point crossing* between the $+/-$ peaks of the S-curve ideally occurs at interferometric null. Note however, that the relative sensitivities of the PMTs and the optical paths traversed by the beam after emerging from the Koesters prism are not identical, and therefore, the zero point crossing may not occur exactly at the interferometric null. (This effect is accounted for in the data reduction process.) Because a one-to-one relationship exists between the rotation angles of the Star Selector A and Star Selector B assemblies and the x,y detector space coordinates, the values of these rotation angles at interferometric null can be used to measure the position of the star in x,y detector space.

Figure 9.6: FGS 3 S-Curves of Upgren69 in F583W at $(x,y) = (0,0)$



Field Dependencies of S-curves

S-curves can be measured anywhere in the FGS FOV. A standard star (UPGREN69) has been observed at nine standard positions within each of the three FGSs. The S-curves obtained from a given FGS are compared among themselves; any variation of the S-curve morphology (its shape) and modulation (its peak to peak amplitude) with position in the pickle is referred to as *field dependency* of the S-curve.

An FGS will display degraded S-curve performance when the collimated beam is not well centered on the face of the Koesters prism. In addition, given the presence of spherical aberration due to the misfigured primary mirror, the wavefront presented to the Koesters prism is not flat but has curvature, a fact that greatly amplifies the effects of optical misalignments. Specifically, a decentered beam in the presence of spherical aberration gives rise to coma and astigmatic aberrations, resulting in degraded S-curve characteristics.

The source of the field dependency is thought to be *beam walk* originating from a misalignment of the star selector B assembly with respect to the Koesters prism that changes as a function of SSB rotation angle. The Star Selectors center the beam on the face of the Koesters prisms while varying the tilt of the wavefront. If there is a clocking error in the alignment of SSB and the Koesters prism, the beam will not remain centered as SSB rotates, resulting in field dependency. Furthermore, if the amount of decentering changes with time, its effects must be monitored in order to calibrate the science data properly. The S-curve measurements in the original three FGSs indicated large decenters of the Koesters prisms in FGS 1 and FGS 2 and strong field dependency in FGS 3.

Figure 9.7 shows that the S-curves of FGS 1 and FGS 2 are not adequate for astrometric science. Only FGS 3 has S-curves with signal-to-noise ratios sufficient for precise astrometry.



The face of the Koesters prism is 50 mm wide. In the presence of spherical aberration from the telescope's primary mirror, a decentering of the wavefront by only 0.25mm will decrease the modulation of the S-curve to 75% of its perfectly aligned value. It has been determined that the decenters in FGS 3 range across the pickle from +0.8 to -0.68 (mm) in x and +0.31 to -0.28 (mm) in y . If the telescope were not spherically aberrated, mis-alignments up to 5 times this size would not be noticeable.

One way to minimize the effects of misalignment and the spherical aberration is to stop down the outer radius of the primary mirror of HST. All the FGSs have a 2/3 pupil stop on their filter wheels. This pupil stop retores the S-curves to a level which allows guiding across the entire pickle. Unfortunately, it also blocks 50% of the target's photons, so nearly a magnitude of sensitivity is lost. Figure 9.8 shows the improvement of the S-curve signature with the 2/3 pupil in place relative to the full aperture for the 3 FGSs at pickle center. Note also the performance of FGS 3 relative to FGS 1 and FGS 2 with full aperture.

Figure 9.7: Full-Aperture X and Y Axis S-curves of Original Three FGSs Measured at the Center of Each FGS Field of View

FGS/9

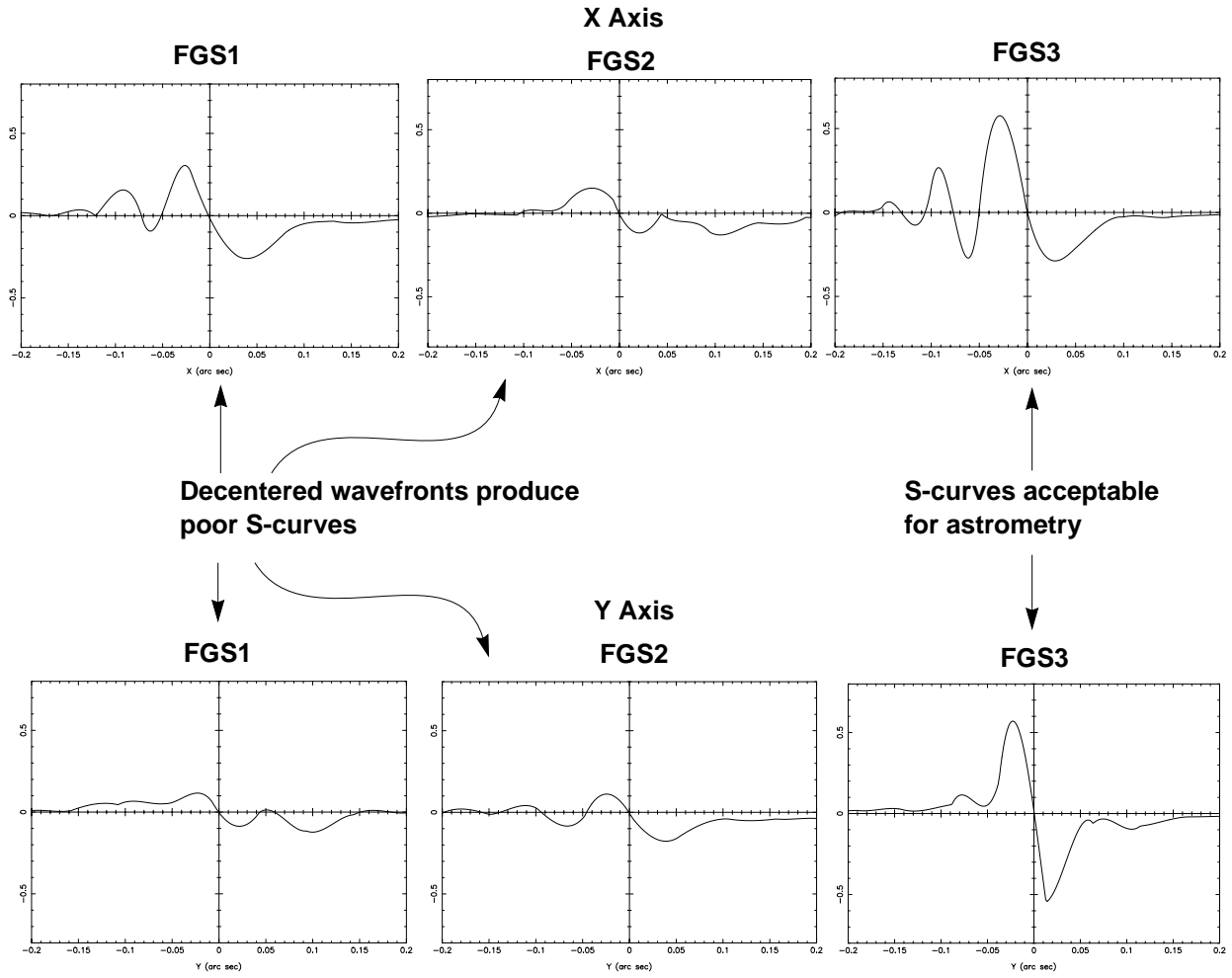
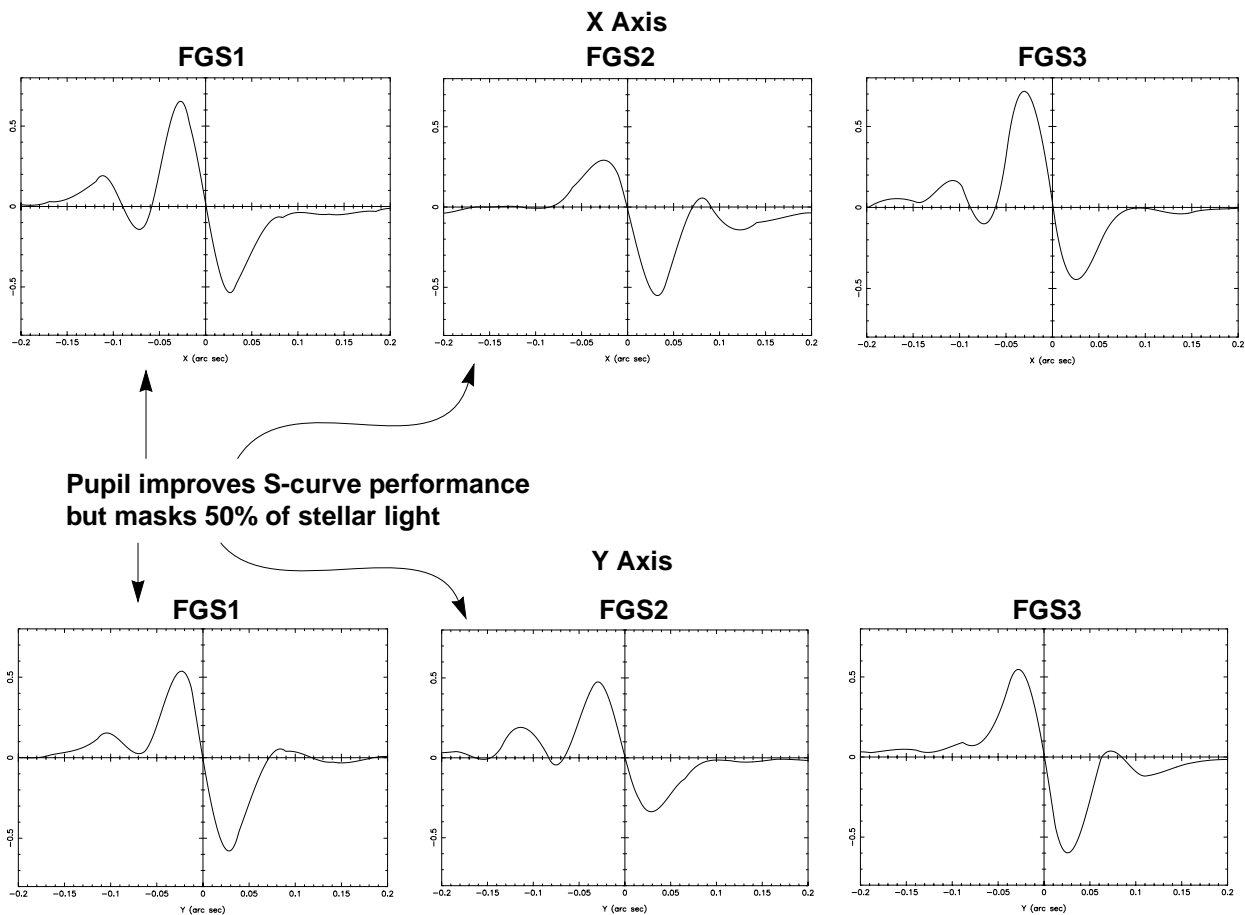


Figure 9.8: Dramatically Improved S-curves for FGS 1 and FGS 2 when Same Star is Observed through the 2/3 Pupil Stop



9.2.4 FGS 1R

The on-orbit evaluations of the FGSs in the presence of spherical aberration from the OTA has shown that proper alignment of the FGS's internal optics is absolutely essential to its performance. Moreover, the apparent decenters of the beams on the faces of the Koesters prisms for the 3 FGSs indicate that the pre-launch alignments within an FGS are not preserved once the instrument arrives in orbit. Therefore, Hughes Danbury Optical Systems, the manufacturer of the FGS, proposed that a refurbished FGS would greatly benefit from a commandable adjustment mechanism that recenters the beam at the Koesters prism. The replacement FGS in radial bay #1, installed on HST during the 1997 servicing mission and referred to as FGS 1R has such a mechanism. In essence one of the static plane fold flat mirrors (FF3) was replaced with an articulating mirror which can be commanded to place the output beam from the Star Selector B assembly at the centers of the two Koesters prisms. Unfortunately, this correction does not fix field dependency because any beam walk from SSB at the

Koesters prism will remain. The FF3 mechanism can center the beam for only one SSB rotation angle.

The FF3 has been adjusted to yield near perfect S-curve performance at the center of FGS 1R's pickle. And although the S-curves of FGS 1R show field dependency, it is not as extreme as that in FGS 3. Therefore, with excellent S-curves at pickle center and improved performance (relative to FGS 3) everywhere else, FGS 1R is potentially the best astrometric science instrument onboard HST. Figure 9.9 and Figure 9.10 compare the S-curves from three positions in the pickle of FGS 3 with those from FGS 1R.

Figure 9.9: Field Dependency of FGS3 Across the Pickle

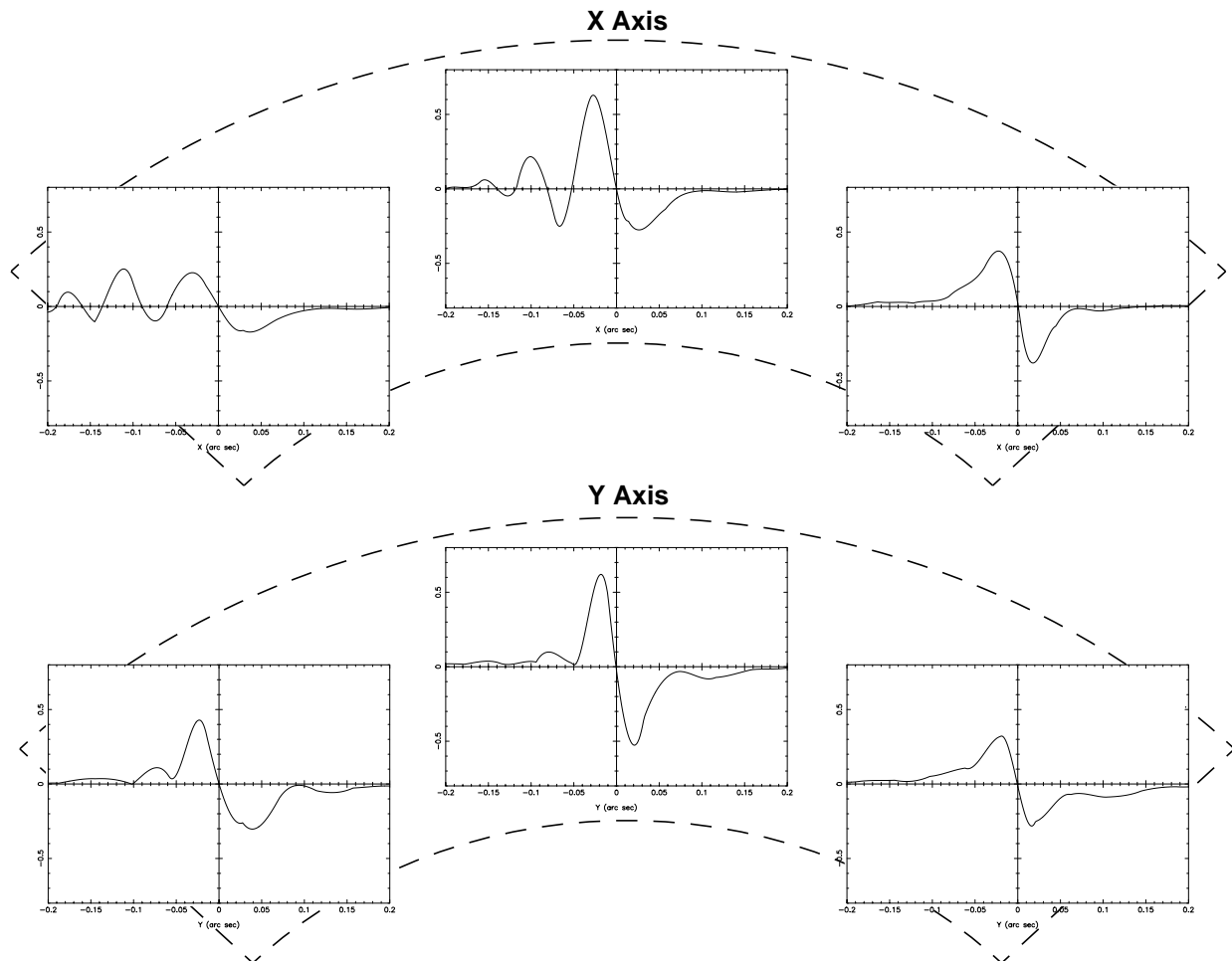
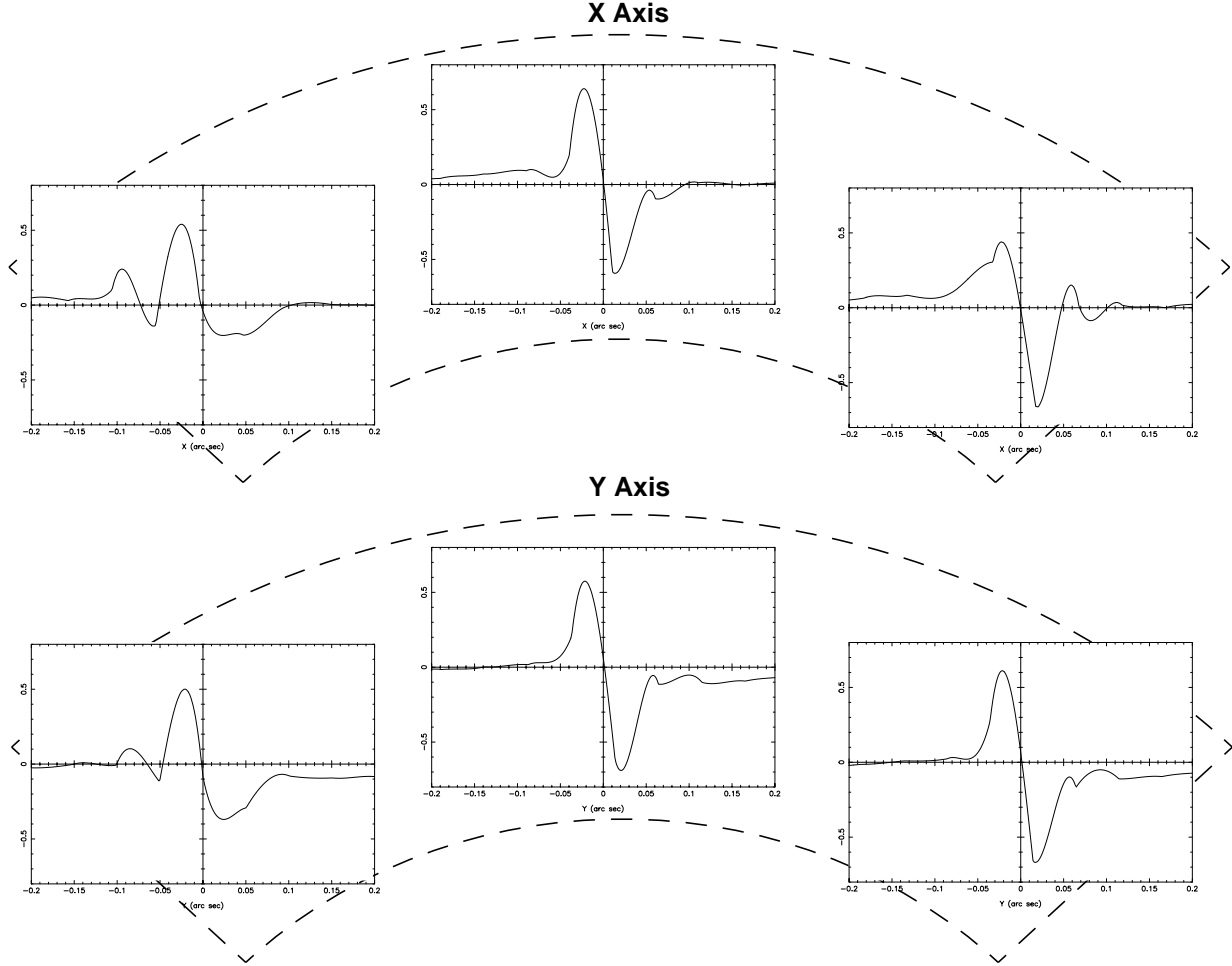


Figure 9.10: Field Dependency of FGS1R Across the Pickle



FGS/9

9.3 FGS Control

Two different kinds of computers can control the three FGSs. One is HST’s housekeeping computer, the DF 224. The other is the Fine Guidance Electronics (FGE) microprocessor associated with each FGS. Both the FGEs and the DF 224 control the FGSs while they are guiding HST. However, when one of the FGSs is being used as an astrometer in POSITION mode, its FGE controls it, and when it is scanning in TRANSFER more, the DF 244 controls it.

The fundamental time interval for an FGS is 25 milliseconds, the shortest time over which the FGSs can compute a fine error signal or respond to commands. Independent of instrument mode or activity, the DF 224 gathers all FGS data at 25 millisecond intervals, assigns them specific locations in the engineering telemetry stream, and downlinks them to the ground. The engineering telemetry format at

the time of transmission determines what FGS data are included in the downlink and the rates at which they are reported.

9.4 Target Acquisition and Tracking

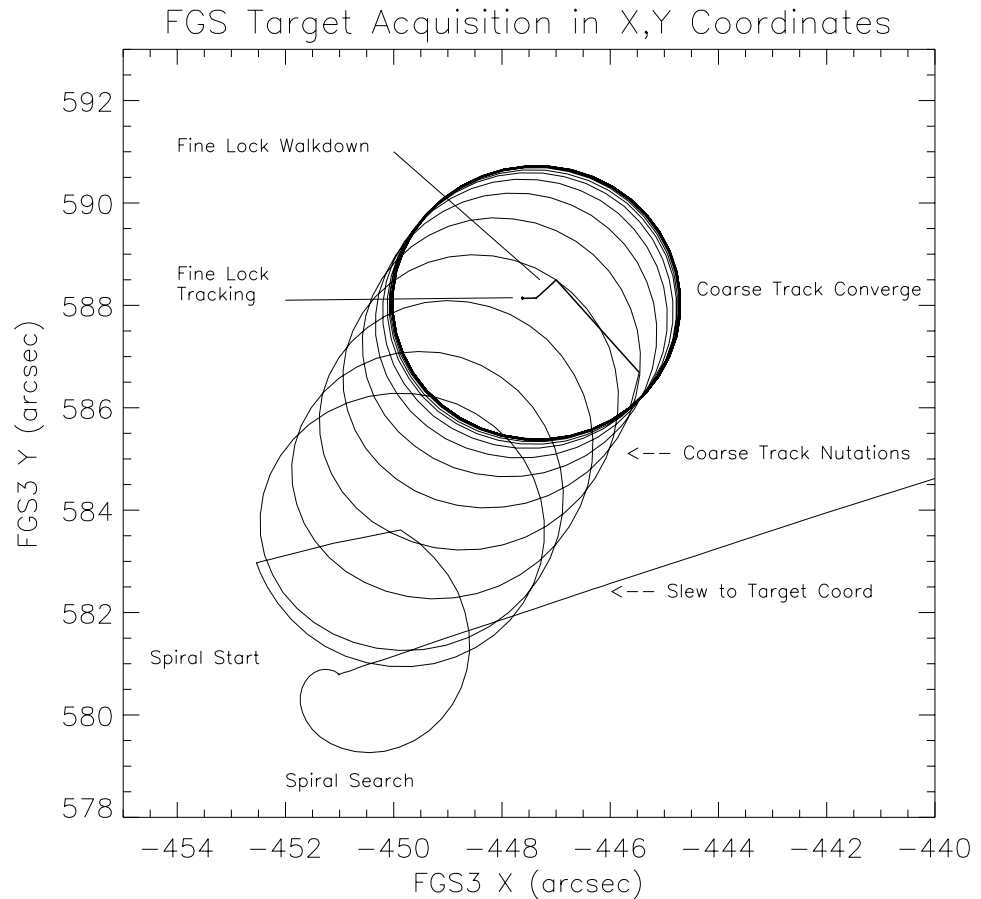
An FGS astrometry dataset contains all the steps in the target acquisition and tracking sequence. This information is necessary because the calibration pipeline uses it in the data reduction process. In this section we describe the acquisition and tracking sequence and define the flags and status bits that record the activities during the acquisition.

The first step in using an FGS either as a guider or an astrometer is to acquire the target in its instantaneous field of view. To accomplish this task, the DF 224 slews the FGS's IFOV to the expected position of the target within its pickle. (Uplinked commands specify the SSA and SSB rotation angles that should put the IFOV on the star.) Once the IFOV arrives at the expected position of the star, the DF 224 delegates control of the FGS to its FGE, which attempts to locate and to track the star by implementing its Search, CoarseTrack, and FineLock algorithms.

Figure 9.11 illustrates the movement of the IFOV during a target acquisition, showing:

1. The end of the slew to the target's expected location.
2. A short spiral search.
3. Coarse track nutations to locate the photocenter.
4. WalkDown to locate interferometric null.
5. Tracking of the star in FineLock.

This particular case was chosen for its clear demonstration of the phases of the acquisition. It is, however, atypical because the 7" difference between the expected location and the true location of the target is unusually large.

Figure 9.11: Location of IFOV as FGS Acquires a Target

9.4.1 Search

The IFOV, under FGE control, steps every 25 msec along an outward spiral while the PMTs count the photons received from the 5" x 5" patch of sky in the IFOV over the same 25 msec. When the counts fall within a specified range, the FGE declares the spiral search a success, and the instrument proceeds to the next phase of the acquisition, CoarseTrack. Otherwise, the FGE continues the spiral search until it either finds the star or completes its maximum search radius, typically 15" for astrometry and 90" for guiding. If no star is detected, the attempt is classified a failure, and the FGE halts further activity.

9.4.2 CoarseTrack

Having successfully completed its SEARCH, the FGE then attempts to acquire and track the star in CoarseTrack. In this mode the FGS determines the photocenter of light by comparing the photon counts from the 4 PMTs as the IFOV nutates in a 5" diameter circular path around the target. Data from each

nutations are used to verify that the star is still in view and to adjust the path of the next nutation to improve the centering of the star. If the FGS is being operated as an astrometer in POSITION mode, the FGE will initiate the FineLock acquisition after a specified number of nutations: 13 for bright, $mv < 14$ objects, 21 for fainter objects. If the FGS is being operated as a guider or as an astrometer in TRANSFER mode, it remains in CoarseTrack until instructed by the DF 224 to initiate an attempt at FineLock.

If the PMT data ever indicate that the star is no longer present, the FGS reverts back to SEARCH mode, beginning where it left off on the search spiral to resume its outward search for the star.

9.4.3 FineLock

Upon completion of the CoarseTrack, either autonomously or by order of the DF 224, the FGE assumes control of the FGS and attempts to acquire the target in FineLock. This activity involves two distinct phases, acquisition and tracking. Both make use of the interferometric signal (the S-curve) to achieve success. The fundamental interval of time during FineLock is the *fine error averaging time* denoted as FESTIME. During an FESTIME the FGS integrates the PMT data while holding the IFOV fixed.

This acquisition phase is called “WalkDown to FineLock,” or simply *the WalkDown*. The FGE commands the FGS’s IFOV to a position offset or “backed-off” from the photocenter (determined by CoarseTrack). The back-off distance, equal in (+dx,+dy), is specified by the uplinked command parameter *KB*:

$$KB = \sqrt{dx^2 + dy^2}$$

For FGS 3 POSITION mode astrometry observations, *KB* is set to 0.3”. For TRANSFER mode observations, *KB* is half the scan length plus an adjustment to compensate for a known bias in the CoarseTrack to FineLock centroids (the difference between the photocenter location and interferometric null).

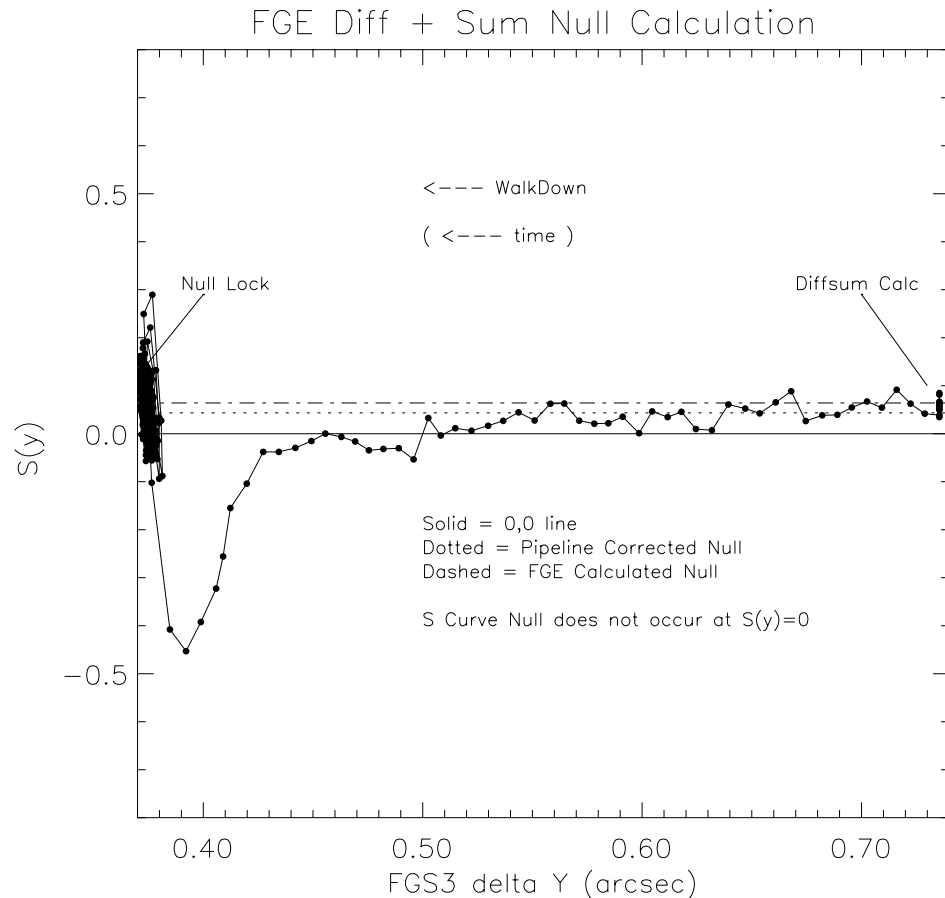
Once the IFOV arrives at the starting point, its position is held fixed for 0.4 SECONDS or an FESTIME, whichever is longer. The FGE collects data from the 2 PMTs on each of the x and y channels to compute an average sum (SUM) and difference (DIFF) on each channel. The DIFF and SUM values compensate for any difference in the response of the two PMTs on a given axis. Thus, the x-axis fine error signal (FES) for the remainder of a POSITION mode observation will be:

$$Q_x = (A_x - B_x - DIFF_x) / SUM_x$$

where A_x and B_x are the average photon counts/25msec (from PMTXA and PMTXB) integrated over the FESTIME, and $DIFF_x$ and SUM_x are the average difference and sum of the PMTXA, PMTXB counts/25msec (determined while the IFOV was held fixed at the starting point of the WALKDOWN). The y-axis FES is computed in a similar fashion. Figure 9.12 shows the instantaneous value of the normalized difference of the PMT counts along the y-axis during a Walk-

Down to FineLock. The fact that the null lies to the positive side of $S_y = 0.0$ clearly demonstrates the need for the DIFF-SUM adjustment to locate the true interferometric null (where $Q_y = 0$).

Figure 9.12: Offset of True Null from $S_y = 0$



During the WalkDown the IFOV creeps towards the photocenter in a series of equal steps, approximately $0.006''$ in x and y , and is held fixed for an FESTIME while the PMT data are integrated to compute the fine error signal on each axis. If the absolute value of the fine error signal for a given axis exceeds a command specified threshold for three consecutive steps, satisfying the *3-hit algorithm*, the FGE concludes that it has encountered the S-curve on that axis. From this point on, a continuous feedback loop between the star selector servos and the value of the fine error signal governs the repositioning of the IFOV along that axis from this point on. The FGS continuously adjusts the star selector positions by small rotations after every FESTIME interval to set the fine error signal to zero, repositioning the IFOV so that the wavefront presented to the face of the Koesters prism has zero tilt.

The FGS tracks the star in FineLock by keeping the IFOV loitering about the star's interferometric null (the zero-point crossing of the fine error signal). Once

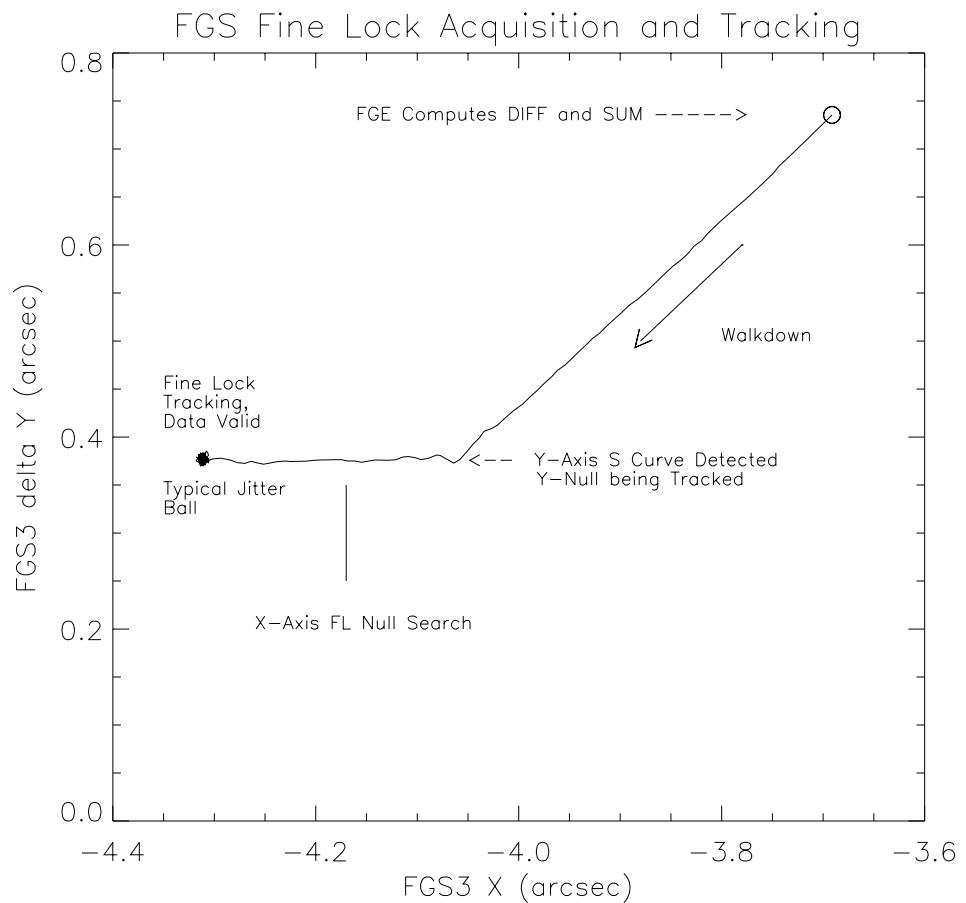
the S-curve has been encountered on, say, the x -axis, the correction to the current position of the IFOV along the x -axis for the next FESTIME is computed by

$$dx = KI_x * Q_x + KO_x$$

where KI_x and KO_x are uplinked command parameters called K-factors.

When the S-curves on both axes have been encountered and have satisfied the 3-hit algorithm, the FGS is said to be tracking the object in FineLock and the FGE sets the DataValid status flag. Figure 9.13 shows the IFOV for both the WalkDown and FineLock tracking in local detector space. Notice that interferometric null is located first along the y -axis, and the IFOV must walk an additional 0.2" along the x -axis to find the x -axis null. This is typical of FGS 3 and is due to the effect of field stop misalignments on the Coarse Track measurements

Figure 9.13: X,Y Position in Detector Space of FGS 3's IFOV During Walkdown to FineLock and Subsequent Tracking of a Star in FineLock



9.5 Transfer Scans

The acquisition of an object for an FGS operating in TRANSFER mode is carried out in the same sequence described above, with the exception that the FGS remains in CoarseTrack until a specified spacecraft time. Thereafter it proceeds to FineLock by slewing the IFOV to the starting point of the first scan. As described earlier for the POSITION mode WalkDown, the FGS averages and differences the PMT data for 0.4 seconds, computes the fine error signal, and compares it to a commanded threshold. However, this threshold equals zero for TRANSFER mode observations, immediately prompting the FGE to declare that FineLock has been achieved and to set the DataValid flag. Setting this flag signals the DF 224 that the FGS is ready to begin the TRANSFER mode observation.

In a TRANSFER mode observation the DF 224 computer steps the FGS's IFOV across the photocenter (determined by CoarseTrack) along a diagonal path in detector space for a distance specified in the original proposal. Each sweep across the target is referred to as a scan. After the completion of a given scan, the IFOV reverses direction and scans the object again until the total number of scans specified in the proposal have been completed. Every 25 msec the PMT data and star selector rotation angles are reported in the telemetry. The FGS samples the entire S-curve, which can be reconstructed by post observation data processing.

9.6 FGS Guiding

When an FGS is used for guiding HST, it acquires a *guide star* in FineLock. The HST pointing control system then corrects telescope's pointing to bring this guide star (by slewing the telescope) to a pre-determined (x,y) position within the pickle of the guiding FGS. Once HST is properly pointed, the FGS continues to track its target in FineLock under control of both the FGE and the DF 224 while the pointing control system monitors the (x,y) position of the guide star and averages that data to determine the current pointing of the telescope. The pointing control system uses these data to eliminate translational and rotational drift of the observatory and to repoint the telescope properly. It also compensates for differential velocity aberration, which is the field-dependent change in the apparent positions of stars owing to the telescope's motion transverse to the direction it is pointed. Because pointing requires two dimensional control, two FGSs are usually used simultaneously to track guide stars. The FGS that controls translational attitude is the *dominant guider*, and the FGS that controls roll is the *roll* or *subdominant guider*.

Sometimes only one FGS actively guides the telescope, maintaining only translational control. Then HST is "free" to roll about the dominant guide star, restrained only by gyroscopic feedback. This situation arises more frequently during astrometry observations than for the other observations because guide star candidates, which can be difficult to find in the first place, are limited to those which appear in two FGSs instead of three.

The FGS astrometry pipeline uses data from the guiding FGSs to provide a high-resolution spatial and temporal HST pointing history over the course of an astrometry observation. These guide star data are useful in both POSITION mode and TRANSFER mode data reductions.

9.7 FGS Astrometry

The two astrometry modes of the FGS are POSITION mode and TRANSFER mode. An FGS in POSITION mode acquires an object in FineLock and tracks it for an extended period of time. An FGS in TRANSFER mode acquires an object and scans the IFOV back and forth along a 45° diagonal path in detector space to sample the interference pattern fully enough to construct an S-curve.

POSITION Mode Observing

POSITION mode observing with the FGS can determine the parallax, proper motion, and/or reflex motion of a given object. A typical POSITION mode observing program, regardless of the scientific goal, measures the (x,y) detector space positions of several objects concurrently observable in FGS's total FOV, or pickle. An FGS can observe only one object at a time, so each of the objects are visited and tracked in FineLock in a sequence specified by the proposal. The DF 224 slews the IFOV of the astrometer to the expected location of the first star in the sequence and relinquishes control to the FGE. The FGE then commands the FGS to acquire and track the target via the Search, CoarseTrack, and FIneLock sequences. Later, at a specific spacecraft clock time, the DF 224 resumes control of the FGS, terminates the FineLock tracking of the object and slews the IFOV to the expected location of the next star in the sequence. This process repeats until the FGS has observed all stars in the observation set belonging to that visit. (The time an FGS tracks a given object in FineLock is usually some 20 seconds longer than the exposure time specified in the proposal because of unused overheads.)

TRANSFER Mode Observing

TRANSFER mode observing with the FGS can resolve the components of multi-star systems and measure the angular dimensions of extended objects. In a TRANSFER mode observation the FGS acquires the object as described above, but instead of attempting to keep the FGS's IFOV at or near interferometric null as in a POSITION observation, the FGS, under control of the DF 224, steps its IFOV is back and forth across the object along a 45 deg diagonal path in detector space, sampling the entire S-curve and its immediate vicinity. Each sweep across the object is referred to as a *scan*. The number of scans, size of each step, and length of each scan are specified in the proposal. Typically, a TRANSFER mode observation will consist of 20 or more scans, each 1.4" long, with a step size of 1 mas.

Mixed Mode Observing

It is sometimes possible to determine the parallax, proper motion, and reflex motion of a multiple star system resolvable by the FGS in TRANSFER mode. If the FGS can both resolve a binary system and measure its parallax, then the

absolute masses of its components would be determined. To accomplish such tasks, the FGS observes the target in TRANSFER mode and other nearby stars in POSITION mode. A mixed mode observing strategy would include a series of POSITION mode observations of the reference stars and a TRANSFER mode observation embedded somewhere in the sequence. Although the post-observation analysis of mixed mode observing data can be challenging, the potential scientific returns have made it an increasingly popular way to use the FGS as an astrometer.

9.8 Astrometry with FGS 3

Among the three FGSs on HST, only FGS 3 has been calibrated and used as an astrometer because the performance of FGS 1 and FGS 2 is not adequate for astrometric science (see “S-curves” on page 9-8). This section will discuss the overall performance characteristics of FGS 3 in both POSITION mode and TRANSFER mode.

POSITION Mode Characteristics

When FGS 3 is used as an astrometer, the “full” F583W wide bandpass spectral filter is used in POSITION mode for stars of $V > 8$ to maximize the sensitivity. The F5ND attenuator is used for stars with $V < 8$. The instrumental properties affecting POSITION mode observation planning and data calibration are: the spatial dependence of the S-curve, the optical field angle distortions across the pickle, and the slow temporal changes in the plate scale, probably due to outgassing of the graphite epoxy. In those areas of the pickle with lower S/N in the S-curve, the limiting magnitude rises from $V = 17$ to $V = 15$. A large area in the central region of the pickle has adequate signal to noise so this problem affects observations only at the edges.

The calibration of optical field angle distortion (OFAD; see “Processing Individual Observations” on page 11-4) involves a fifth-order two-dimensional polynomial fit to observations of an astrometric standard field. The measured coordinates of a target are corrected in the pipeline using the transformation defined by these polynomial coefficients. The temporal changes to the plate scale and the OFAD are monitored on a monthly or bi-monthly basis via observations of a standard astrometric field and are provided as updates to the calibration database. In spite of the field dependent behavior of FGS 3, the repeatability and hence the accuracy of individual POSITION mode measurements of stars distributed throughout the pickle is typically about 1.5 mas for $V < 14.5$ and about 2 mas for fainter objects. These numbers are determined from the residuals of plate overlays in which the pickle’s orientation on the sky is constant from plate to plate, so that field-dependent (OFAD) corrections do not enter. However, when the OFAD correction is required, the overall pickle-wide error budget increases to about 2.7 mas.

TRANSFER Mode Characteristics

The S-curves of FGS 3 display strong field dependency on both the x and y axis. Each of these S-curves is nearly ideal at one location in the pickle, but the

optimal position for the x axis does not coincide with that for the y axis. This lack of coincidence has affected the astrometric performance of FGS 3 because science observations in TRANSFER mode are executed at only one position, pickle center. Any other position could be used, but pickle center was chosen as an optimal compromise and is the only position in FGS 3 supported by the TRANSFER mode calibration database. The y -axis sports a nearly ideal S-curve, while that on the x -axis suffers from aberrations.

Because the x -axis has the degraded S-curve, it is the limiting factor in the TRANSFER mode performance of FGS 3. When the projected angular separation of a binary system along the x -axis is less than about 20 mas, it is not resolved on the x -axis. On the other hand, the y -axis has been shown to resolve systems with separations as small as 10 mas. (The success at resolving the individual components depends, of course, on the magnitude difference: the larger the delta magnitude, the more difficult the observation.) This suggests that FGS 1R, with its nearly ideal S-curves on both axis at the same place in the pickle (at the center), should be able to resolve binary systems with separations on the order of 10 mas, and perhaps to detect structure in an object at the 5 mas level.

FGS Data Structures

In This Chapter...

Engineering Telemetry Data / 10-1
FGS Astrometry Files / 10-2
Relationship to Phase II Request / 10-6
Jitter Files / 10-6
SMS Support Data / 10-7

This chapter describes how to identify and interpret the contents of FGS data files. An FGS dataset received from the Archive contains information from all three FGSs, plus some supporting data on the spacecraft itself. These files arrive in FITS format and need to be converted to GEIS format as described in Chapter 2 before processing.

10.1 Engineering Telemetry Data

The FGS is unique among HST's science instruments in that its data downlink is carried on the engineering data stream rather than the science data stream. FGS data are transmitted with the engineering data because the FGSs are controlled by the spacecraft's housekeeping computer, consistent with their primary role as part of the pointing control system. While the contents of the downlink for the other science instruments depend upon the specifics of that instrument, the contents and rates of the FGS data are determined by the engineering telemetry format.

The fundamental FGS data of interest for astrometry and guiding are:

- The photon counts from the four photomultiplier tubes.
- The instantaneous values of the two Star Selector servo angles.
- The twelve status flag bits.

The first two items are sampled every 25 msec, while the status flag bits are reported every 150 msec for the FN format (100 msec for HN). Additional FGS

mnemonics present in the telemetry either can be reconstructed from those listed above or are of interest only to the system engineering staff.

When an FGS is operated as an astrometer, the Astrometry and Engineering Data Processing (AEDP) system, part of HST's ground support system at Goddard Space Flight Center (GSFC), extracts specific FGS mnemonics from the engineering telemetry and builds the astrometry data products. These are similar to the GEIS format files produced for the other science instruments (see Chapter 2 for more on GEIS file format). This system also accesses the Mission Support Schedule (MSS) and inserts additional information into various header keywords necessary for proper identification and interpretation of the associated data files.

As of late November 1997, generation of the astrometry data products will become the task of OMS's AST subsystem at STScI. The Astrometry and Engineering Data Processing system will then be phased out.

10.2 FGS Astrometry Files

Each FGS astrometry observation generates header and data files (.a*h/.a*d) for all three FGSs whenever any one FGS, generally FGS 3, is used as an astrometer. The contents of the data files for the guiding FGSs, generally FGS 1 and 2, record the photometry and positions of the two guide stars. The contents of the header files contain both information common to all FGSs and information specific to the FGS associated with that file, such as the values assigned to uplinked control parameters.

File Description

The data from the FGS mnemonics included in the astrometry subset are extracted from the telemetry stream and organized into groups. The data are grouped by type and mnemonic (e.g., group 5 contains the positions of star selector A). The GEIS data file for a given FGS contains 17 groups of data of which only seven are of interest for astrometry science data processing. The other ten groups continue to exist for traditional and historic reasons. We anticipate that later versions of the OMS AST subsystem will generate data files with only the necessary seven data groups.

Each individual FGS astrometry observation produces one GEIS header and data file pair for each of the three FGSs. A typical FGS POSITION mode observing sequence or *visit* consists of an HST orbit filled with observations of several stars, usually the science target and a few reference stars. Therefore, each visit will yield a number of GEIS file sets for three FGSs, each set corresponding to an observation of an individual star. These file sets contain all the FGS tracking and photometry data from the time interval when the specific observation was made.

The rootnames of FGS data sets adhere to the IPPSSOOT convention described in Chapter 2. The first letter is always an F, identifying the file as FGS data, and the last letter is an M, indicating that the data were merged real time and tape recorded. For example, an FGS observation might be named f42n0203m. If

5 individual FGS observations were made in this hypothetical visit, their rootnames would be f42n0201m, f42n0202m, f42n0203m, f42n0204m, and f42n0205m. The 02 in each case is the visit number, which is important to note because all observations from a given visit must pass through the data reduction pipeline together (see Chapter 3). The two digits following the visit number give the observation numbers, in the sequence they were obtained.

For each observation, there should be six files, one header-data pair for each FGS. Data from the first observation will appear in the following files

Header	Data	Sensor
f42n0201m.a1h	f42n0201m.a1d	FGS 1
f42n0201m.a2h	f42n0201m.a2d	FGS 2
f42n0201m.a3h	f42n0201m.a3d	FGS 3

In this example, if FGS 3 is the astrometer and measures the position of a star in exposure id = F42N0201M, then the f42n0201m.a3h and f42n0201m.a3d files contain the astrometry data. The guide star data gathered during this astrometry observation are recorded into files f42n0201m.a1h, f42n0201m.a1d and f42n0201m.a2h, f42n0201m.a2d for FGS 1 and FGS 2 respectively.

Group Structure and Group Contents

Each data file contains the same number of data groups (17) and each group is of the same size, having the same number of samples. The duration of the observation and the rate of the most frequently read out mnemonic determine the sizes of the groups for a particular observation (the photon counts and star selector positions are readout 40 times per second). If an observation spans 100 seconds, then each data group will have:

$$100 * 40 = 4000 \text{ samples}$$

Some groups, such as the flags/status bits group, are readout less frequently (once every 150 msec). In this situation the valid data are packed from the beginning and the remaining 5/6 of the group is padded with fill data.

For FGS astrometry science data processing, the groups of interest in each GEIS data file are groups 1 through 6 and group 17. Table 10.1 lists the contents of these groups. :

Table 10.1: Groups in FGS GEIS Files

Group	Contents	Description	Sample Period
1	PMTXA	Photon counts, channel A, <i>x</i> -axis	25 msec
2	PMTXB	Photon counts, channel B, <i>x</i> -axis	25 msec
3	PMTYA	Photon counts, channel A, <i>y</i> -axis	25 msec
4	PMTYB	Photon counts, channel B, <i>y</i> -axis	25 msec
5	SSENCA	Star selector A encoder position	25 msec
6	SSENCB	Star selector B encoder position	25 msec
17	FLAGS/STATUS BITS	Indicates specific activity of FGS	150 msec

Groups 1 through 4 contain the photometry data for the 5" x 5" patch of sky observed by the FGS. If the FGS is guiding and tracking its guide star, then it registers the photon counts from the guide star. If the FGS is operating as an astrometer, there will be an astrometric target in its instantaneous field of view (IFOV) only after the IFOV has slewed to the target's position and the FGS has successfully acquired the star. While the slew is underway, the FGS records the sky background and serendipitous field stars. These background data are used in the data reduction pipeline.

Groups 5 and 6 record the position (to 0.6 mas) of the IFOV in the FGS's pickle and therefore in the HST focal plane. If the FGS is guiding, the measured position of the guide star is fed into the Pointing Control System so that the spacecraft's pointing can be maintained or corrected. These guide star data are used in the pipeline processing discussed in Chapter 11.

The flags/status bits group records the value of the 12 flags and indicators, each of which is a single bit which is either set (=1) or not set (=0). If the FGS is guiding and is tracking its guide star in FineLock, then the FineLock, DataValid, and Star Presence flags will be set (=1) and all others not set (=0). The astrometer FGS will display a sequence of flags/status bits settings which reflects the current activity of the FGS. If the FGS is to be operated in POSITION mode, then the following sequence of flag/status bits would be displayed for a successful acquisition:

Table 10.2: Status/Flag Bits

SSM	SR	CT	FL	DV	SP	Action
ON						Slewing the IFOV to star's location
	ON					Begin spiral search for star
	ON				ON	Spiral search located star
		ON			ON	Star detected, begin CoarseTracking
		ON		ON	ON	CoarseTracking successful
			ON		ON	Attempt FineLock acquisition
			ON	ON	ON	Tracking star in FineLock

The flags and status bits have the following meanings when set to 1:

- **SSM:** FGS under control of DF 224 computer.
- **SR:** FGS in autonomous (FGE) control, performing a spiral search .
- **CT:** FGS in CoarseTrack mode.
- **FL:** FGS in FineLock mode, if DV=0, then in WalkDown phase, if DV=1, then tracking in FineLock.
- **DV:** CoarseTrack or FineLock was successful.
- **SP:** Star presence, photon counts summed from all four PMTs fell within the commanded range (LOCOUNT < PMTSUM < HICOUNT).

When determining the position of an astrometric object observed in FineLock, the data of interest to the astrometry pipeline are:

- The slew to the star's expected location (provides background data).
- The WalkDown to FineLock (provides critical PMT data to better locate interferometric null) and to support FGS photometry.
- The FineLock tracking of the object (provides the FGS's measured location of star in focal plane).

More details on interpreting and making use of the FGS data are provided in the sections "Plate Overlays" on page 13-3 and "Resolving Structure with TRANSFER Mode" on page 13-5.

FITS Header Keywords

The GEIS header files for FGS data contain keywords that will help to interpret the data files. The most important keywords contained in the header files are:

```

NAXIS      :   number of dimensions in the data file (=1 of FGS)
NAXIS1     :   number of samples (or pixels) in each data group
GCOUNT     :   number of groups in the data file (=17 for FGS)
BITPIX     :   bits/pixel (=32 for FGS)
DATATYPE   :   datatype (= 32 bit integer for FGS)
FGSID      :   identifies astrometer FGS
FGSNO      :   identifies FGS associated with this header file
    
```

```

PASTMODE:    observing mode, POSITION or TRANSFER
AUTOS       :    actual start time of observation (Universal time)
PRAV1      :    predicted right ascension of HST's V1 axis
PDECV1     :    predicted declination of HST's V1 axis
PROLLV3    :    predicted roll orientation of HST
PRATGT     :    predicted right ascension of target
PDECTGT    :    predicted declination of target
PX_POS     :    HST state vector (position and velocity) at
PY_POS     :    beginning of observation (at PUTOS)
PZ_POS     :
PX_VEL     :
PY_VEL     :
PZ_VEL     :
CAST_FLT   :    filter used for the observation.

```

The values assigned to these keywords are used in the calibration pipeline processing discussed in Chapter 11. To print an entire header to the screen, you can use the IRAF **imheader** task as in the following example:

```
cl> imheader f42n0201m.a1h long+ | page
```

10.3 Relationship to Phase II Request

Associated with each astrometry observation is the Support Schedule file, with suffix `.dmh`. This product is generated at STScI by the Science Planning and Support System (SPSS). It is a GEIS header file with no associated data file. Contained within are keywords and values which repeat some of the information in the FGS header files, such as the HST state vector. More importantly, the contents of this file can be used to map a specific FGS observation to the proposal's Phase II exposure log sheet. The proposal ID, PI identifier, target name, proposal type, proposal title, and exposure logsheet line are among the entries. The only keyword used by the astrometry pipeline is the value of `DGESTAR` to determine which guiding FGS was tracking the dominant guide star. Observers should review the contents of both the `.a3h` and `.dmh` files, which can be done using **imheader** as above.

10.4 Jitter Files

Since about October 1994 the Observatory Monitoring System (OMS) has been populating the STScI data archives with the Observation Logs (see Chapter 2 and Appendix C). They are of secondary use for the processing of FGS astrometry data because the guide star data are directly available to the astrometry pipeline. The item of interest in the `*.jih` file is the OMS computed HST roll angle. Recall that the `.a*h` header files contain the predicted roll angle. The details of how the telescope is pointed on the sky reveal that the roll angle is not set by the pointing control system using FGS data, rather it is set using less accurate fixed

head star tracker data. Whatever roll angle results is then maintained by the roll guide star. OMS uses the FGS data, guide star RA, Dec, and HST/FGS alignment matrices to compute the actual roll of the telescope, which can differ from the predicted roll by as much as 0.4 degrees. The more accurate OMS roll angle is best used for the final computation of astrometric parallaxes and binary star position angles.

See the OMS documentation on the Web where the accuracies of roll calculation, etc. are discussed. The URL is:

http://www.stsci.edu/ftp/instrument_news/Observatory/taps.html

10.5 SMS Support Data

The FGS is unique among the science instruments onboard HST in that its total field of view (the pickle) is large and therefore sensitive to the effects of differential velocity aberration (DVA), the field-dependent shifts of star positions owing to the telescope's component of motion in the direction it is pointing. It is possible to maintain the pointing of HST so that the effects of DVA can be compensated for, but only at one place in the focal plane—the *alignment point*. Because typical FGS astrometry programs measure the relative positions of stars spread widely throughout the pickle, there can be at most only one star that will not suffer from DVA. Although this effect is potentially large, up to 20 mas, it is relatively simple to correct for this aberration. The algorithm requires HST's V1 pointing, V3 roll, and state vector, all obtained from the .a*h header files, plus the specification of the alignment point. The alignment point data for all FGS observations are stored in a reference library maintained by the STScI FGS staff. The data originate from the Science Mission Schedule (SMS) and are automatically extracted and entered into this library. The astrometry pipeline accesses this library when the differential velocity aberration connection is made.

Chapter 11

FGS Calibration

In This Chapter...

The Visit / 11-1
Initial Data Processing / 11-2
POSITION Mode Pipeline / 11-3
TRANSFER Mode Pipeline / 11-7
POSITION Mode Pipeline Output / 11-8

This chapter describes how FGS data are calibrated. Unlike the data from other HST instruments, FGS astrometry data are not calibrated automatically. Observers now require the assistance of the FGS team at STScI and the Space Telescope Astrometry Team (STAT) at the University of Texas to process astrometry science data through the FGS pipeline. However, efforts are underway at STScI to provide IRAF/STSDAS tools that will enable observers to easily calibrate data using the current best set of calibration reference files and algorithms. These tools may eventually evolve into a fully automatic pipeline that generates and archives calibrated FGS astrometry data. Check STScI's FGS web pages for updates.

STScI acknowledges the contribution of the STAT in the design, development, and maintenance of the astrometry data processing pipeline. This pipeline has been in use since the beginning of the HST mission and has evolved into a robust and reliable tool that has processed more than 7,000 individual FGS astrometry observations.

11.1 The Visit

The current pipeline requires all data from a single visit to reside in a dedicated directory. The required files are the GEIS files for all three FGSs (.a*h/ .a*d), the support schedule file (.dmh), and a pointer to the HST alignment point library. For example, if the FGS visit to be analyzed comprises five individual astrometry observations, then the directory containing the data to be calibrated should contain files shown in Table 11.1 (where PPP and SS are place holders for

the actual program_ID and visit ID, respectively). There should be 35 files (5 observations, each with 7 files).

Table 11.1: GEIS Files in an FGS Dataset

File Name	Contents
fpppps01m.a1h	Header file, FGS1
fpppps01m.a1d	Data file, FGS1
fpppps01m.a2h	Header file, FGS 2
fpppps01m.a2d	Data file, FGS 2
fpppps01m.a3h	Header file, FGS 3
fpppps01m.a3d	Data file, FGS 3
fpppps01m.dmh	Support schedule for observation 01
...	...
fpppps05m.a1h	Header file for FGS 1
fpppps05m.a1d	Data file for FGS 1
fpppps05m.a2h	Header file for FGS 2
fpppps05m.a2d	Data file for FGS 2
fpppps05m.a3h	Header file for FGS 3
fpppps05m.a3d	Data file for FGS 3
fpppps05m.dmh	Support schedule for observation 05

11.2 Initial Data Processing

When all of the files pertaining to a given astrometry visit are present in a single directory, pipeline processing can begin. The initial round of data processing accomplishes several general tasks, regardless of whether the observations were gathered in POSITION mode or TRANSFER mode. The pipeline:

1. Reads the seven GEIS files belonging to each individual observation.
2. Identifies the FGS being used for astrometry and its observing mode.
3. Identifies potentially missing files.
4. Determines the status of the guiding FGSs, checking whether zero, one, or two guiding FGSs were actively maintaining the pointing of the telescope and whether they were guiding in CoarseTrack or FineLock.
5. Inspects the flags/status bits to determine whether the astrometry observation succeeded or failed, and in the case of a failure, to identify the reason for the failure.
6. Prepares output files with keywords whose values are either extracted from the input header files or computed from contents of the data files.

7. Assesses the data quality of successful observations, masking outliers, garbled telemetry, and telemetry dropouts. (Outliers are data that do not appear to be garbled but make no sense when viewed in the context of neighboring data points.)

11.3 POSITION Mode Pipeline

The pipeline usually calibrates POSITION mode data in two distinct stages. The first stage processes each single observation in a stand-alone fashion, ignoring the other observations belonging to the same HST visit. The second stage relates all the individual observations to one another so that an astrometric “plate” can be produced. Here we describe the sequence of events recorded during a POSITION mode observation and then the two stages of POSITION mode data calibration. See page 11-8 for a sample of POSITION mode pipeline output.

11.3.1 Position Mode Observations

In a typical POSITION mode observing program the astrometry FGS sequentially observes in Fine Lock *several* stars distributed about the pickle. Any temporal variability in the telescope pointing will contaminate the measured relative positions of these targets. Thus, the measured positions of all targets must be mapped onto a common, fixed coordinate system before an astrometric plate can be assembled.

Experience has shown that FGS astrometry is sensitive to HST body *jitter* and FGS *drift*. The jitter can be eliminated using the guide star data, whereas the drift is removed by applying a drift model derived from *check star* data. A *check star* is a target observed multiple times during the visit. Typically the observing strategy should involve at least two check stars, and they should be observed at least three times each.

The dataset for a given observation includes the Slew to the target, the Search, the CoarseTrack, the WalkDown, and the FineLock tracking, as well as guide star data over the same interval of time. These data provide information used by the pipeline algorithms to determine backgrounds, to locate the interferometric null, and ultimately, to pinpoint the position of the star relative to the other stars observed in the visit. These data can also be used for photometric studies.

The Slew portion of the observation is used to measure the background. During the slew the astrometer's photomultiplier tubes count the photons in the 5" IFOV, registering the background and serendipitous stars. These star spikes are removed in the pipeline's background averaging process, via a trimmed mean.

Upon completion of the slew, the FGS microprocessor assumes control and begins the acquisition of the target as described in “Target Acquisition and Tracking” on page 9-16. After the completion of CoarseTrack, the DataValid and TransferHold flags are set to 1. Then the FineLock acquisition begins and the DataValid flag returns to zero until tracking in FineLock begins and the DataValid

flag is set once again (see Table 10.2). The FGS will continue to track its target in FineLock until the DF 224 computer terminates the activity and slews the IFOV to the next target in the sequence. This process repeats for each exposure until the end of the visit.

When the target is faint or the data are noisy, the onboard DIFF, SUM algorithm suffers from poor photon statistics and therefore might cause the FGS to mis-identify true interferometric null. The pipeline corrects for this problem using PMT data gathered during the slew, WalkDown, and FineLock tracking as described in step 5 below.

11.3.2 Processing Individual Observations

POSITION mode pipeline processing for each individual observation in the visit executes the following steps:

1. Inspection of the flags/status bits to locate the data fields recording:
 - The slew of the IFOV to the target's location.
 - The WalkDown to FineLock.
 - The FineLock tracking (FineLock/DataValid) of the target .
2. Computing the centroid of the IFOV, taken to be the median of the instantaneous x,y positions during the FineLock/DataValid interval, in the astrometer as well as the guide star positions in the guiding FGSs. Standard deviations about these centroids are also computed.
3. Updating the HST state vector, specified in the header files for the beginning of the observation, so that it is accurate for the temporal midpoint of the FineLock/DataValid interval.
4. Gathering photon statistics on:
 - PMT background during the slew to the target.
 - PMT data taken while the IFOV was still far ($>0.1''$) from the null. (These data can be used to calculate SUM and DIFF values more accurate than those computed at the start of the WalkDown because they are based on up to 80 times more samples.)
 - PMT data taken while FGS was in FineLock/DataValid. (These data are averaged to compute the points on the S-curves of both axes which the FGS's microprocessor determined to be the true interferometric null. These values should be approximately the same as the DIFF, SUM computed by the FGS's microprocessor at the start of the WalkDown).
5. Applying the DIFF and SUM corrections to both axes of only the astrometry data to locate the true interferometric null. This algorithm determines the slope of the fine error signal near interferometric null as a function of position in the pickle, using a library of reference S-curves, the target magnitude, making use of the background data computed above, and the difference in the photomultiplier averages computed during the WalkDown and the FineLock/DataValid intervals (see Figure 9.12). This correction tends to

be small for bright stars ($V < 13.5$) but can be as large as 5 mas for faint ($V > 15$) stars.

6. Converting the raw telemetry encoder positions to instantaneous x,y detector coordinates using several parameters, such as the star selector lever arm lengths, and offset angles. The lever arm and offset angle are known to vary in time. They are monitored by an ongoing program called the Long Term Stability Monitor (LTSTAB) which executes multiple times a year. The values applied in the pipeline are determined by interpolation of the LTSTAB results.
7. Correcting the x,y centroids in the astrometer for Optical Field Angle Distortions (OFAD).
8. Correcting distortions in the astrometer arising from the pickoff mirror and aspheric mirror.
9. Removing differential velocity aberration from the x,y centroids using the updated HST state vector, a JPL Earth ephemeris, HST's V1 RA and DEC, the V3 roll, and the V2,V3 position of the alignment point. This correction is applied to both the astrometer FGS and the guide star FGSs.

The pipeline produces output files that log these corrections, the associated standard deviations about the centroids, and the photometry averages from the four PMTs.

At this point no further processing on the individual observations are possible. The next step is to combine the measurements of the individual targets to correct for POSITION-mode jitter and FGS drift.

11.3.3 Assembling the Visit

The goal of this segment of the pipeline is to map all of the positional measurements of the individual targets onto a fixed but arbitrary coordinate system. It involves POSITION mode *de-jittering* and application of the DRIFT correction.

POSITION Mode De-jittering

The pipeline accounts for spacecraft jitter during the visit by establishing a fixed but arbitrary reference frame determined by the x,y centroids of the guide stars within the guiding FGSs. The HST pointing control system uses the position of the dominant guide star to fix HST's translational position and that of the roll guide star to fix HST's orientation. The output products of the pipeline processing of the individual observations include the x,y centroids of the guide star positions evaluated over the same time interval as the astrometer centroids. During the course of the visit any change in the x,y centroids of the dominant guide star within its FGS is interpreted to be HST translational jitter and is removed from the both the astrometer and the guide star maintaining HST roll. Next, any motion of the roll guide star with respect to the dominant guide star perpendicular to the line between them is interpreted as uncompensated roll of HST about the dominant guide star. The pipeline then removes this roll from the astrometry data. Typically the size of the de-jittering correction is less than a millisecond of arc when

averaged over the visit but can be as large as 3–5 mas for any given observation, such as when HST transits from night into day.

De-jittering is not performed at a 40 Hz rate because that would introduce noise into the dataset. Instead the time-averaged centroids of the guide stars are computed for the same time interval that the astrometer was in FineLock/DataValid. The positions of the guide stars in the first exposure, corrected for differential velocity aberration, define the reference frame for the remainder of the visit. So, for example, if the dominant guide star x,y centroids measured during the N th astrometry observation differed from those in the first observation by $(dx,dy) = (1 \text{ mas}, 1 \text{ mas})$, then the appropriate conversion to $dV2, dV3$ is applied to the roll star and the astrometer's local x,y centroids. This procedure creates a fixed but arbitrary coordinate system for the entire visit.

POSITION Mode Drift Correction

After the FGS data have been de-jittered, there will remain an apparent motion of those astrometry targets which have been observed more than once within the observing sequence. These check stars provide the data required for the next and potentially large correction. The drift correction model assumes that the astrometer is a rigid body which both translates and rotates in the HST focal plane during the course of the visit and corrects the measured positions of the stars in the visit for contamination by this motion.

The time-tagged positions of the check stars are used to generate a model for this drift, and the time-tagged positions of all the stars in the visit are adjusted by application of the model. Three separate models can be applied:

- **Linear:** Translation only, no rotation.
- **Quadratic:** Translation only, no rotation.
- **Quadratic and roll:** Translation and rotation.

The choice of model depends upon the number of check stars available and the number of times each is observed. Clearly if there is only one check star in the visit the rotation model cannot be applied. Also, if check stars are not observed frequently enough (three times or more), the quadratic models might not be reliable. The pipeline applies all three models, providing three sets of corrected centroids. It is the responsibility of the GO to decide which set is best. The output of the fitting program includes fit residuals and χ^2 .

The size of the drift correction is typically 6 to 12 mas under two-FGS guidance. The amount of drift appears to be related to the intensity of the bright Earth projected down the V1 boresight during target occultations. This intensity, and hence check star drift (generally), is highest for targets in HST's orbital plane and lowest for those at high inclination.

When only one FGS is used for guiding, the telescope is not roll-constrained. Under such circumstances the check stars can reveal very large motions, up to 60 or 70 mas over the course of the orbit. Nevertheless, this drift can be successfully removed from the astrometry data, provided the proposal contained an adequate check star scenario. For example, the overlay of the plates from two separate POSITION mode visits, each measuring some 20 stars in an astrometric field

distributed throughout the pickle yielded an rms residual of about 1 mas, even though one of the visits had one-FGS guiding and check-star drifts on the order of 30 mas.

The Data Analysis chapter (Chapter 13) discusses the techniques of plate overlays and determinations of parallax and proper motion.

11.4 TRANSFER Mode Pipeline

11.4.1 TRANSFER Mode Dataset

The dataset for a TRANSFER Mode observation includes all of the acquisition phases described in “Target Acquisition and Tracking” on page 9-16, as well as the transfer scans described in “Transfer Scans” on page 9-21. Each TRANSFER mode observation consists of a number of scans specified in the original proposal. Simultaneous guide star data cover the entire observation.

Automatic pipeline processing of TRANSFER mode data is limited to locating each scan in the astrometer’s data file, editing out bad data arising from garbled telemetry, and determining the median position and standard deviations of the guide stars within the guiding FGSs during each scan.

The pipeline generates three ASCII files for every scan, one for each FGS. Each file contains the 40 Hz raw star selector A,B encoder values and the photon counts/25msec of the four PMTs. The guide star data are provided for (optional) de-jittering of the astrometer’s IFOV. Each of these files begins with a small header containing keywords whose values pertain globally to the observation or specifically to the scan, such as the filter used or the universal time at the start of the scan. The HST state vector is also included.

11.4.2 Mapping TRANSFER Mode to POSITION Mode

Planned upgrades to the TRANSFER mode pipeline to support the mapping of the TRANSFER mode results onto POSITION mode plates, along with POSITION mode observations made in the same visit, include the following steps:

1. Differential velocity aberration correction to the astrometer and the guide stars. This step requires access to the definitive HST orbit file because the HST state vector evolves considerably over the course of the TRANSFER mode observation, which can be up to 40 minutes long.
2. Computation of guide star x,y centroids to establish the fiducial position for the dominant guide star.
3. Translational de-jittering of the astrometer IFOV at 40 Hz.
4. Location of the individual scans in the observation.

5. Cross-correlating, shifting, binning, and co-adding the individual scans.
6. Polynomial curve fitting to the co-added scans. The residual of each scan to this fit is evaluated to locate individual scans which might be contaminated by HST jitter. (Step 3 would not remove a recentering event in which the guider was not tracking its guide star during some extreme HST jitter crises). Such scans are identified and disqualified, and steps 5 and 6 are iteratively repeated until no further disqualifications occur.
7. Time tagging and recording the shifts determined from the cross-correlation. These data are used to generate a drift model for the TRANSFER mode data when the observation is in a visit with POSITION mode observations.
8. Generation of output files that log the corrections made, identify the scans which have been disqualified, specify the polynomial coefficients of the fit, and present the drift model and guide star centroids and standard deviations. This step also includes creation of individual scan files which contain the star selector A,B values and the counts from the four PMTs for each scan. These files have names such as F42N0102M.nSm where $n = 1,2,3$ to identify the FGS and $m=1,2,3,\dots$ to specify the scan number.

11.4.3 Limitations of the TRANSFER Mode Pipeline

The pipeline cannot carry out further processing of TRANSFER mode data because the header and data files made available to the pipeline do not contain sufficient information. For example, the header files do not specify if the observation is of a single calibration reference star, or of a binary system, or an extended object, each of which needs different additional processing. The B-V color of the target needs to be specified for the analysis of observations of binary stars or extended objects so that the appropriate single star reference S-curve can be retrieved from the calibration library. These activities will be discussed in Chapter 13.

Observers should consult the STScI FGS web pages for updates to the status of the pipeline upgrades.

11.5 POSITION Mode Pipeline Output

The following example illustrates the current format of the output from the POSITION mode pipeline, which gives the key information needed for data analysis. Enhancements of this format are under development.

```
!
!   CALFGS:    VERSION 2.0
!   date of calibration processing -> 18-FEB-97  15:44:29
!
!
OBSERVATION_ID = F3FV0602M      !
OBSERVING_MODE = POSITION        !
```

```

TARGET_ID      = 6920_975          !
STAR_ID        = 0                 !
MAGNITUDE      = 12.85            !
PRA            = 92.22249166667    ! degrees, predicted target position
PDEC           = 24.38458055556    ! degrees, predicted target position
!
RAV1           = 92.28756740940    ! degrees ... Spacecraft pointing data
DECV1          = 24.58115491606    ! degrees
ROLLV3         = 87.69312835639    ! degrees
X_POS          = 6255.850861       ! Km ..... Spacecraft orbital position
Y_POS          = 2940.146717       ! Km
Z_POS          = -937.186147       ! Km
X_VEL          = -3.271298         ! Km/sec ... Spacecraft orbital velocity
Y_VEL          = 5.872820         ! Km/sec
Z_VEL          = -3.460530         ! Km/sec
OBS_TIME       = 1997 031 12:47:46 ! UT at (X,Y,Z,Vx,Vy,Vz)
!
ASTROMETER_FGS = 3                 ! ID of astrometer FGS
FILTER          = F583W            ! ASTROMETER FGS FILTER
DISTORTION      = PERFORM          ! status: PERFORM, OMITT, or COMPLETED
LATERAL_COLOR   = PERFORM          !
WEDGE           = PERFORM          !
ABERRATION      = PERFORM          !
!
! *** POSITION from encoder values (-2=FGS data corrupted or not available)
!           (FL)           (FL)           (FL)
X_AVE          = -201.3386  -161.9243   191.5194   ! asec, FGS=1,2,3
Y_AVE          = 795.5815   643.5501   716.0092   ! asec, FGS=1,2,3
X_X_AVE        = 0.0020     0.0021     0.0028   ! asec, FGS=1,2,3
Y_Y_AVE        = 0.0023     0.0017     0.0026   ! asec, FGS=1,2,3
X_Y_COR        = 1.611E-01  1.513E-01  1.034E-01  ! asec, FGS=1,2,3
X_Y_COV        = 7.395E-07  5.304E-07  7.656E-07  ! asec, FGS=1,2,3
!
X_MEDIAN        = -201.3386  -161.9242   191.5194   ! asec, FGS=1,2,3
Y_MEDIAN        = 795.5815   643.5503   716.0091   ! asec, FGS=1,2,3
X_MAD           = 0.0016     0.0016     0.0021   ! asec, FGS=1,2,3
Y_MAD           = 0.0018     0.0014     0.0021   ! asec, FGS=1,2,3
!
! *** positions valid only after DISTORTION & ABERRATION corrections ***
!
X_CORRECTED    = -201.3161  -161.8805   191.4970   ! asec, FGS=1,2,3
Y_CORRECTED    = 795.5054   643.5306   716.0089   ! asec, FGS=1,2,3
X_X_CORRECTED  = 0.0020     0.0021     0.0028   ! asec, FGS=1,2,3
Y_Y_CORRECTED  = 0.0023     0.0017     0.0026   ! asec, FGS=1,2,3
!
RA              = -1.0000     -1.0000     -1.0000   ! deg FGS=1,2,3
DEC             = -1.0000     -1.0000     -1.0000   ! deg FGS=1,2,3
!
EXPOSURE_TIME   = 4.06500E+01     ! seconds of FINELOCK DATA (POSITION MODE)
NPIXELS         = 1627             ! # samples used from FINELOCK interval
!
!
! ..... !
!
! PCS ALIGNMENT PARAMETERS FOR DIFFERENTIAL VELOCITY DE-ABBERATION
!
VELAB_SI        = FGS
VELAB_FGS       = 3
X_VELAB         = -253.72
Y_VELAB         = 712.47
!
DOM_GS_FGS      = 2
!

```

```

! ..... !
!
!           GUIDE STAR / ASTROMETER TRACKING
!
!           FGS1           FGS2           FGS3
!
!           GUIDE STAR     GUIDE STAR     ASTROMETER
!           FINE LOCK       FINE LOCK       FINE LOCK
!
! ..... !
!
!           PHOTOMETRY: average counts/25 msec over exposure interval
!
!           GUIDE STAR     GUIDE STAR     ASTROMETER
!           FGS1           FGS2           FGS3
!
PMTSUM      =      831.6524      5843.9882      649.6138
PMTXA       =      187.9005      1355.9204      160.2842
PMTXB       =      175.9104      1254.1306      167.2680
PMTYA       =      235.8850      1742.8638      165.0006
PMTYB       =      231.9565      1491.0734      157.0609
!
PMTXA_BCK_MED = 4.00 ! astrometer bckgrnd MEDIAN of PMTXA (-1=NA)
PMTXB_BCK_MED = 5.00 ! astrometer bckgrnd MEDIAN of PMTXB (-1=NA)
PMTYA_BCK_MED = 4.00 ! astrometer bckgrnd MEDIAN of PMTYA (-1=NA)
PMTYB_BCK_MED = 4.00 ! astrometer bckgrnd MEDIAN of PMTYB (-1=NA)
!
PMTXA_BCK_AVE = 3.98 ! astrometer bckgrnd AVERAGE of PMTXA (-1=NA)
PMTXB_BCK_AVE = 4.71 ! astrometer bckgrnd AVERAGE of PMTXB (-1=NA)
PMTYA_BCK_AVE = 4.69 ! astrometer bckgrnd AVERAGE of PMTYA (-1=NA)
PMTYB_BCK_AVE = 4.10 ! astrometer bckgrnd AVERAGE of PMTYB (-1=NA)
!
PMTXA_BCK_MAD = 2.77 ! astrometer bckgrnd MAD of PMTXA (-1=NA)
PMTXB_BCK_MAD = 3.26 ! astrometer bckgrnd MAD of PMTXB (-1=NA)
PMTYA_BCK_MAD = 3.38 ! astrometer bckgrnd MAD of PMTYA (-1=NA)
PMTYB_BCK_MAD = 3.02 ! astrometer bckgrnd MAD of PMTYB (-1=NA)
!
PMTXA_BCK_SIG = 1.40 ! astrometer bckgrnd S.D. of PMTXA (-1=NA)
PMTXB_BCK_SIG = 1.73 ! astrometer bckgrnd S.D. of PMTXB (-1=NA)
PMTYA_BCK_SIG = 1.73 ! astrometer bckgrnd S.D. of PMTYA (-1=NA)
PMTYB_BCK_SIG = 1.48 ! astrometer bckgrnd S.D. of PMTYB (-1=NA)
!
PMTXA_BCK_TMIN = 2.00 ! astrometer bckgrnd trimed MIN for PMTXA (-1=NA)
PMTXB_BCK_TMIN = 2.00 ! astrometer bckgrnd trimed MIN for PMTXB (-1=NA)
PMTYA_BCK_TMIN = 2.00 ! astrometer bckgrnd trimed MIN for PMTYA (-1=NA)
PMTYB_BCK_TMIN = 2.00 ! astrometer bckgrnd trimed MIN for PMTYB (-1=NA)
!
PMTXA_BCK_TMAX = 7.00 ! astrometer bckgrnd trimed MAX for PMTXA (-1=NA)
PMTXB_BCK_TMAX = 8.00 ! astrometer bckgrnd trimed MAX for PMTXB (-1=NA)
PMTYA_BCK_TMAX = 8.00 ! astrometer bckgrnd trimed MAX for PMTYA (-1=NA)
PMTYB_BCK_TMAX = 7.00 ! astrometer bckgrnd trimed MAX for PMTYB (-1=NA)
!
SAMPLES_BCKGD = 1006 ! no. of samples used to compute background
!
PMTXA_WD_MED = 165.50 ! astrometer walkdown MED for PMTXA (-1=NA)
PMTXB_WD_MED = 164.00 ! astrometer walkdown MED for PMTXB (-1=NA)
PMTYA_WD_MED = 164.00 ! astrometer walkdown MED for PMTYA (-1=NA)
PMTYB_WD_MED = 160.00 ! astrometer walkdown MED for PMTYB (-1=NA)
!
PMTXA_WD_AVE = 165.43 ! astrometer walkdown AVE for PMTXA (-1=NA)
PMTXB_WD_AVE = 163.68 ! astrometer walkdown AVE for PMTXB (-1=NA)
PMTYA_WD_AVE = 165.38 ! astrometer walkdown AVE for PMTYA (-1=NA)
PMTYB_WD_AVE = 159.98 ! astrometer walkdown AVE for PMTYB (-1=NA)
!

```

```

PMTXA_WD_MAD = 11.19 ! astrometer walkdown MAD for PMTXA (-1=NA)
PMTXB_WD_MAD = 11.63 ! astrometer walkdown MAD for PMTXB (-1=NA)
PMTYA_WD_MAD = 11.98 ! astrometer walkdown MAD for PMTYA (-1=NA)
PMTYB_WD_MAD = 10.75 ! astrometer walkdown MAD for PMTYB (-1=NA)
!
PMTXA_WD_SIG = 13.89 ! astrometer walkdown S.D. for PMTXA (-1=NA)
PMTXB_WD_SIG = 14.48 ! astrometer walkdown S.D. for PMTXB (-1=NA)
PMTYA_WD_SIG = 14.85 ! astrometer walkdown S.D. for PMTYA (-1=NA)
PMTYB_WD_SIG = 13.11 ! astrometer walkdown S.D. for PMTYB (-1=NA)
!
NSAMPLES_X = 376 ! X AXIS: #SAMPLES USED TO COMPUTE WD PMT DIFF/SUM
X_FL_DIFF/SUM = -0.0219 ! X PMT DIFF/SUM FROM FLDV INTERVAL (-1=NA)
X_WD_DIFF/SUM = 0.0055 ! X PMT DIFF/SUM FROM WALKDOWN INTERVAL (-1=NA)
K1X_UPGREN69 = 0.0301 ! REF X AXIS S-CURVE INVERSE SLOPE OF UPGREN69
X_DIFF = -0.000824 ! X CENTROID SHIFT (ARCS), ADD TO X_MEDIAN (-1=NA)
!
NSAMPLES_Y = 241 ! Y AXIS: #SAMPLES USED TO COMPUTE WD PMT DIFF/SUM
Y_FL_DIFF/SUM = 0.0253 ! Y PMT DIFF/SUM FROM FLDV INTERVAL (-1=NA)
Y_WD_DIFF/SUM = 0.0171 ! Y PMT DIFF/SUM FROM WALKDOWN INTERVAL (-1=NA)
K1Y_UPGREN69 = 0.0151 ! REF Y AXIS S-CURVE INVERSE SLOPE OF UPGREN69
Y_DIFF = 0.000125 ! Y CENTROID SHIFT (ARCS), ADD TO Y_MEDIAN (-1=NA)
!
! ..... !
!
! COARSE TRACK coordinates
!
! GUIDE STAR GUIDE STAR ASTROMETER
! FGS1 FGS2 FGS3
!
CT_X = -124.846 -69.454 191.867 ! X, arc seconds
CT_Y = 705.588 720.397 716.168 ! Y, arc seconds
!
! ..... !
!
! raw, STAR SELECTOR values mean and median over measured interval
! (-2=mean, median not computed), (FL) = finelock, (CT) = COARSE TRACK
!
! GUIDE STAR GUIDE STAR ASTROMETER
! FGS1 (FL) FGS2 (FL) FGS3 (FL)
!
SS_A_AVERAGE = 0 0 0 ! "THETA A"
SS_B_AVERAGE = 0 0 0 ! "THETA B"
SS_A_MEDIAN = 499751 376375 258989 ! "THETA A"
SS_B_MEDIAN = 713495 830629 616509 ! "THETA B"
SPCR1 = 768442 734328 518064 ! "CT THETA A"
SPCR2 = 1560040 1479462 1232352 ! "CT THETA B"
!
!
! ..... !
!
! Star Selector to X,Y conversion parameters
!
! FGS1 FGS2 FGS3
!
SS_A_dev_angle = 6.885174200 6.759527300 6.852572700
SS_B_dev_angle = 6.862490000 6.772780000 6.857440000
SS_A_offset = -0.049323366 0.568665570 -0.627579600
SS_B_offset = 0.000000000 0.000000000 0.000000000
magnification = 57.219718800 57.236389900 57.043404000
!

```


FGS Error Sources

In This Chapter...

Levels of POSITION Mode Errors / 12-1
Observation-Level POSITION Errors / 12-2
Visit-Level POSITION Errors / 12-11
Field-Level POSITION Errors / 12-13
TRANSFER Mode Errors / 12-14

The previous chapters have described TRANSFER mode and POSITION mode observations. Some FGS error sources are mode-specific, while others are common to both modes. This chapter discusses those uncertainties, both statistical and systematic, which remain after the pipeline calibrations of raw POSITION mode and TRANSFER mode observations. Each step in the calibration procedure leaves its own residuals which contribute to the overall error budget.

The increasingly common use of the FGS astrometer for mixed-mode observations, in which TRANSFER mode and POSITION mode observations are made in the same visit, combines the errors associated with each mode and introduces new sources as well. The next chapter discusses the analysis of mixed-mode observations and the associated errors.

12.1 Levels of POSITION Mode Errors

An FGS in POSITION mode measures the relative angular separations of several objects. The objects generally will be separated by angles on the order of arc minutes, will range over several magnitudes in brightness (possibly from $V = 3$ to 17), and will have different B-V colors. Because their parallaxes and proper motions need to be determined, HST will visit a given astrometric field several times, spanning perhaps two to four years or longer, over the course of an observing program. During each visit, the FGS will track each target in FineLock, one at a time, according to the instructions and sequence specified in the proposal.

Sources of error in these POSITION mode measurements can be categorized into three distinct levels:

- **Observation level:** errors associated with each individual FineLock acquisition and tracking sequence.
- **Visit level:** errors involved in constructing a virtual plate for a given FGS astrometric visit.
- **Field level:** errors that arise when comparing virtual plates of the same field taken during different visits.

Errors from lower levels will percolate through to the top.

12.2 Observation-Level POSITION Errors

An individual observation in POSITION mode acquires a single target in FineLock and tracks it for a specified period of time. The goal of the observation is to pinpoint the target's location in FGS detector space. Pipeline processing of POSITION mode data (see "POSITION Mode Pipeline" on page 11-3) converts the Star Selector A,B encoder angles into detector space (x,y) coordinates for the three FGSs and computes the median of these values over the period of time when the object was being tracked in FineLock by the astrometer. It then adjusts the astrometer's (x,y) centroid using data gathered by the four photomultiplier tubes (PMTs) during the slew of the IFOV to the target (to measure the background and dark counts), the WalkDown to FineLock, and the FineLock tracking of the object. This adjusted centroid is subsequently corrected for optical field angle distortion (OFAD), the aberration of the aspheric mirror, the cross filter effect if applicable (see page 12-9), and finally, differential velocity aberration. Here we address the errors remaining after these steps.

12.2.1 Rotation Angle Errors

The FGE reads rotation angles of the Star Selector A and B assemblies as 21-bit integers. The 14 most significant bits are determined by optically reading an absolute binary code pattern, while the 7 least significant bits are derived from an optical resolving device that reads a special encoder disk pattern that generates a quadrature set of sinusoidal signals. A correction to the 7 least significant bits leaves an uncertainty in the (x,y) values estimated to be about ± 0.3 mas owing to noise and non-repeatability of the optical reader. The corrections to the 14 most significant bits are absorbed in the optical field angle distortion (see below) and therefore do not contribute here.

12.2.2 Centroiding Errors

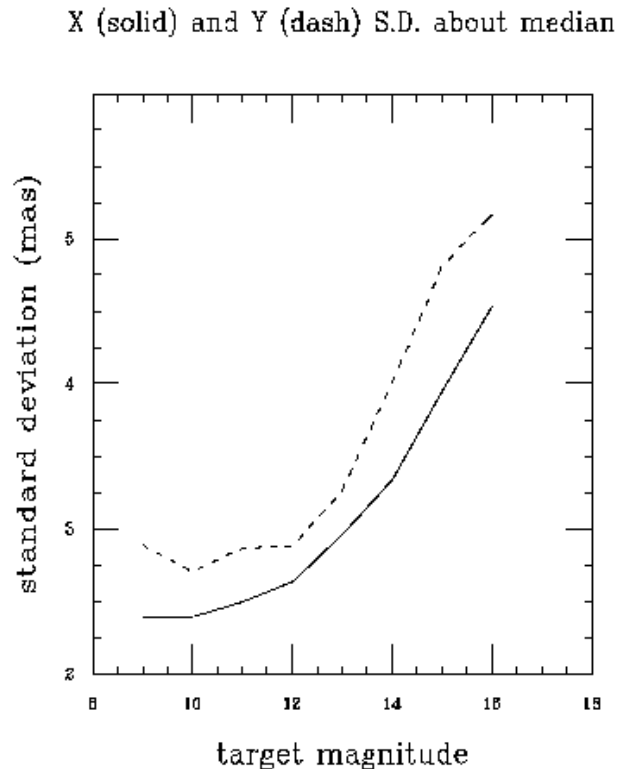
During nominal FineLock tracking of an object, the instantaneous field of view of the FGS will jitter and drift about the (x,y) median over time scales not shorter

than the fine error signal averaging time (FESTIME) and as long as the low frequency vibrational modes of the spacecraft (up to 40 seconds). The standard deviation of these excursions depends upon the magnitude of the target and HST vehicular jitter.

Target Magnitude

Because the FGS tracks an object by computing and implementing corrections to the current position of the IFOV on the basis of the fine error signal, noise in the PMT counts can introduce errors in the corrections. To compensate for the increase of the photometric noise for fainter targets, the FESTIME is increased to boost the signal/noise of the fine error signal. This adjustment not only yields fewer independent samples of the target's position but also results in more sluggish tracking. For example, a 320s exposure of a 17th magnitude object having an FESTIME = 3.2s generates only about 100 independent measurements of the target's position, while an observation of the same duration of a 9th magnitude object with FESTIME = 0.025s yields 12800 independent samples. In addition, as the FESTIME increases, the rms excursions of the IFOV about the interferometric null tend to be larger because the FGS responds more slowly to the high frequency HST vibrational modes (faster than 0.1 Hz). Figure 12.1 plots the standard deviation about the x and y centroids of 5000 stars measured in FineLock as a function of the target's magnitude. Note how steeply the standard deviation rises past $V > 12$.

Figure 12.1: Standard Deviation of IFOV about Median (x,y) Position as Function of Target Magnitude



The standard deviation of the FineLock tracking is not a direct measure of the observation's accuracy—it is the repeatability of the centroiding that reflects the observation's reliability. The pipeline computes the centroids over segments of the exposure, and it is the dispersion of these values that should be used to assess accuracy. Generally, the repeatability is about 1 mas for $V < 14.5$, increasing to about 2 mas for $V = 16$.

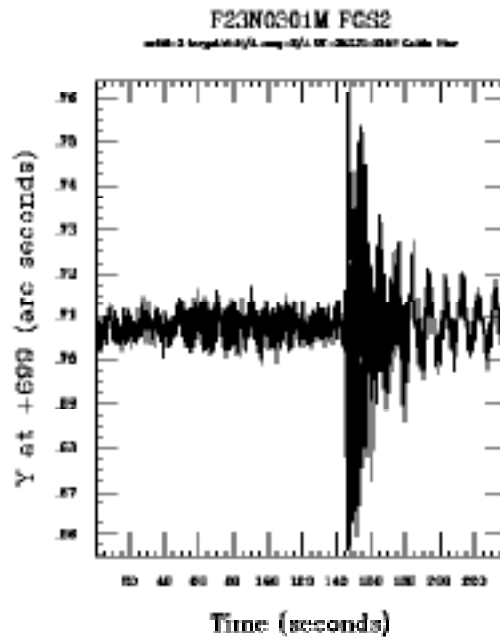
Vehicular Jitter

Analysis of both the guide star and astrometry data can reveal how successfully HST's pointing control system guided the spacecraft and stabilized its attitude during an observation. The guiding FGSs track their guide stars in FineLock, so their centroids and standard deviations can be computed and compared to those from the astrometer for identical intervals of time. The centroids of all three FGSs will show some jitter owing to the magnitude effect discussed above. However, the pointing control system is designed to minimize the impact of the internal jitter in the guiding FGSs on the pointing of the spacecraft, and for the most part, it succeeds. The jitter of bright astrometry targets is not systematically higher than that of the guide stars.

Nevertheless, transient events during the course of an observation can jitter the telescope, introducing additional noise in the tracking of the guide stars and the astrometry target. For example, as HST moves from orbital day to night or night to day, its solar panels undergo large temperature changes that excite HST's vibrational modes. These vibrations increase the standard deviations of FineLock tracking in the three FGSs by up to a factor of eight over the pre-transition values. Some events actually cause a small (5 mas) but significant temporary repointing of the telescope.

Figure 12.2 shows how night-to-day transitions can affect HST's pointing. The excited vibrational modes of HST are readily apparent and contrast sharply with the quiescence of normal guiding seen prior to the transition. This extreme case clearly demonstrates how such terminator crossings can induce significant spacecraft jitter.

Figure 12.2: Guide Star Motion in FGS 2 Before and During Night-to-Day Transition



Spacecraft jitter had been a major problem for astrometry observations during the first three years of the mission. The FGSs could not reliably hold the guide stars in FineLock over the span of the visit, and once lost, the guide stars for astrometry observations would not be recovered for the remainder of the orbit. However, improvements to both the pointing control system, in January 1993, and the solar panels, replaced in the first servicing mission, have reduced spacecraft jitter to a mild nuisance in the astrometry data reduction process which is well handled by proper application of the guide star data.

12.2.3 Locating Interferometric Null

The discussion of the acquisition of an object in FineLock (page 9-18) pointed out that the FGE attempts to eliminate differences in the responses of the two PMTs on a given channel by computing their average difference (DIFF) and average sum (SUM) at the starting point of the WalkDown to FineLock. For the remainder of the WalkDown and tracking in FineLock, the fine error signal is computed making use of these values, as described on page 9-18.

The quality of this correction to the fine error signal depends in part on the errors in the determinations of DIFF and SUM, which depend in turn on the target magnitude and the integration time used to compute them. For bright stars ($V < 12.5$) the FESTIME is 25 msec and the DIFF, SUM values are computed from 16 25msec intervals (0.4 sec). On the other hand, the FESTIME for a 13th magnitude star is 50 msec, but the DIFF, SUM integration time remains at 0.4 sec, so only 8 FESTIME intervals are represented. Table 12.1 shows the FESTIME and DIFF, SUM integration times as a function of target magnitude. The important point to

note is that as target magnitude increases, fewer FESTIME integrations are included in the evaluation of the DIFF and SUM. The values in this table are representative; actual FESTIME values depend on the filter and mode in use.

Table 12.1: FESTIME and DIFF, SUM Integration Times as a Function of Target Magnitude

Magnitude	FESTIME (seconds)	DIFF/SUM Integration Time (seconds)	# of FESTIMES Represented in DIFF/SUM
9	0.025	0.4	16
10	0.025	0.4	16
11	0.025	0.4	16
12	0.025	0.4	16
13	0.050	0.4	4
14	0.200	0.4	1
15	0.400	0.4	1
16	.800	0.8	1
17	3.200	3.2	1

As targets become fainter, the FGE applies increasingly unreliable DIFF and SUM values in its calculation of the fine error signal and therefore risks locking onto a region of the S-curve which is not the true interferometric null. Figure 9.12 shows an example of the segment of an S-curve sampled during a WalkDown to FineLock. In this case, the FGS's estimate of the fine error signal's value at null is not quite correct. Pipeline processing can determine the true null more accurately by using the WalkDown data to calculate better values of DIFF and SUM. The following values go into the adjustment of the median (x,y) centroid of the astrometer for this effect:

- The average counts / 25 msec of each PMT during the WalkDown, before the S-curves are detected.
- The average counts / 25 msec of each PMT during the FineLock tracking of the star while the FGS tracks what it believes is true interferometric null.
- The background contribution to the PMT counts.
- A reference S-curve providing the slope of the S-curve near null.

The size of the correction computed by the pipeline is small for bright stars but can be large for faint ($V > 15$) stars, up to 5 mas.

Each of the four components specified above contribute to the formal error associated with this adjustment. Errors from the first two depend on the number of photons counted during the WalkDown and the FineLock tracking. The error associated with the third also depends upon the number of photons registered while the background and dark counts were being evaluated, but note that these counts do not have a Poissonian distribution. The S-curve correction, which

accounts for the field dependency of FGS 3's S-curves, interpolates the slopes of S-curves at nearby locations in the pickle, measured in a calibration program, to estimate the S-curve at the target's location.

Clearly the overall uncertainty of this correction will depend strongly upon the magnitude of the star and less sensitively on the exposure time. Table 12.2 provides estimates of this error as a function of target magnitude for a typical POSITION mode observation and background. These estimates assume that 80 *x*-axis WalkDown steps and 40 *y*-axis WalkDown steps were available for PMT averaging and that the target was tracked in FineLock for 60 sec.

Table 12.2: Estimated DIFF/SUM Correction Error as a Function of Target Magnitude

Magnitude	Error (mas)	
	X-axis	Y-axis
10	< 1	< 1
12	< 1	< 1
13	< 1	< 1
14	1	1
15	1.5	2
16	2	2
17	> 2	> 2

12.2.4 Optical Field Angle Distortion

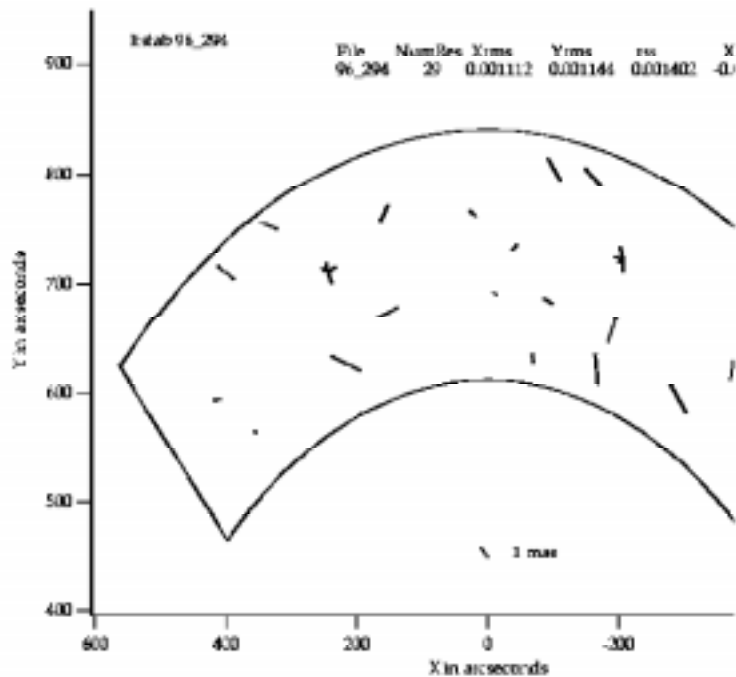
Optical field angle distortion (OFAD) alters the measured relative angular separations of stars distributed across the FGS's pickle from their true angular separations. This distortion originates from both the FGS/OTA optical train and errors in the 14 most significant bits of the 21-bit Star Selector A and B encoder values. Correcting for this distortion is absolutely necessary for all POSITION mode observing programs that visit the target field at a variety of HST orientations (roll angles). The Space Telescope Astrometry Science Team has made extensive efforts to calibrate optical field angle distortion and to maintain this calibration.

This correction is independent of target magnitude, color, or exposure time, and depends only upon the location of the object within an FGS's detector space. Residuals from the calibration itself indicate how well it accounts for this uncertainty in POSITION mode observations. In an OFAD calibration, the FGS observes a field of stars at several different HST pointings and roll angles. Measured changes in the angular separations of these stars as a function of the telescope's orientation on the sky must be a signature of the instrument itself.

Because no ground-based astrometric catalog of adequate accuracy exists for calibrating the FGS, the OFAD calibration program must simultaneously and self-consistently generate a 2 mas star catalog while deriving the distortion

correction. Comparisons of this star catalog, taken to represent the true positions of the stars, with the individual FGS observations, corrected according to the derived distortion model, reveal the accuracy of the correction itself in terms of the residuals that remain. This procedure is analogous to the simpler case of fitting a line to a distribution of points and computing the standard deviation of the points along the line to determine the quality of the fit. In this case, the star catalog corresponds to the line, while the corrected star positions correspond to the points. Because of boundary effects and the distribution of the stars in the pickle that were observed in the calibration proposal, the smallest residuals occur in the central region of the pickle, with larger residuals near the edges or extreme azimuthal ends. In the area where most astrometry science observations are made, residuals are typically slightly more than 1 mas per axis, suggesting that the uncertainty of a given measurement is about 1.5 mas. Toward the pickle edges and azimuthal extremes, the errors can become as large as 3 to 4 mas. Figure 12.3 shows a plot of the residuals from the OFAD calibration as a function of position in the pickle of FGS 3. The residuals shown can be attributed both to small errors in the catalog and to errors in the OFAD calibration.

Figure 12.3: Comparison of Observed Star Positions (Corrected for OFAD) with Cataloged Star Positions (Derived from OFAD Calibration)



12.2.5 Lateral Color Error

The chromatic response of the five element corrector group, the polarizing beam splitter, the filter, and the Koester prisms, introduces a slight color dependence into the tilt of a wave front measured by the FGS. This chromatic effect results in both a displacement of the target's position in the FGS's field of

view and stretching of its S-curve. The effect on the S-curve is important for TRANSFER mode observing and will be discussed in “Resolving Structure with TRANSFER Mode” on page 13-5. The displacements of greater concern are POSITION mode observations. If left uncorrected, these will result in an apparent HST roll-dependent motion of the star with respect to the background reference stars of different color.

Two on-orbit attempts to calibrate this lateral color effect directly have been made. These tests were largely unsuccessful, owing to the poor distribution of reference stars, strong reliance on the OFAD corrections, and small sizes of the lateral color shifts. Ground based tests were conducted prior to installing FGS 3 on HST, but because these did not use a spherically aberrated beam, and because launch and gravity release significantly affected FGS 3’s internal alignments, those measurements are not considered to be reliable and therefore are not used in the calibration.

As stated above, the lateral color effect will masquerade as roll-dependent motion of an object if it has a color temperature significantly different from that of the reference field. The size and sign of this effect as a function of color difference are not well understood. It is suspected to be important only when the color differences exceed one magnitude, where it is estimated to be about 1 mas.

12.2.6 Cross Filter Effect

The cross filter calibration addresses the apparent change in the measured position of an object observed in POSITION mode as function of the filter selected for the observation. As with the lateral color effect, any shift, if unaccounted for, will result in an apparent HST roll-dependent motion of the object relative to those stars measured through a different filter.

The FGS filter wheel can be rotated to bring any one of five different filters into the optical path. Of these filters, generally only the F583W and F5ND are used in POSITION mode astrometry. The other, full-aperture filters, F550W and F605W have not been used because their spectral band passes offer no observing advantage over the wide bandpass F583W. The F5ND is actually an attenuator of approximately five magnitudes rather than a filter, and it is used when the target is too bright to be observed with the F583W filter.

Occupying the 5th slot on the wheel is the PUPIL. It is not a filter but rather a 2/3 pupil stop. Use of the pupil significantly reduces the degrading effect of spherical aberration but collaterally alters the field dependence of the distortions. Consequently, the OFAD calibration for the F583W filter cannot be applied to PUPIL observations. And because there are no OFAD calibrations for the PUPIL, it is not supported in POSITION mode for science observations.

Because POSITION mode astrometry uses only the F583W and F5ND filters, only these two need be compared for the cross filter calibration. The calibration program itself was a three orbit test which measured the position of a bright ($V = 8.08$) star at three locations in the pickle. The position of the star was measured in each orbit by alternate observations using the F583W and the F5ND, for a total of 12 pairs (24 observations). The shifts were found to be different at each of the

three locations, indicating a field dependent response. The shifts were also larger than expected, up to 7 mas in x and y , but the formal errors of the test were small, at about 1 mas.

Because of the field dependency of the cross filter calibration and the paucity of locations (three) within the pickle where it has been measured, it is risky to apply these large corrections to data collected at any other position in the pickle. Nearly all science observations that require this correction use the F5ND filter at pickle center, a location supported by the calibrations. In such fortunate cases, the uncertainty of the measurement is about 1 mas.

12.2.7 Differential Velocity Aberration

Differential velocity aberration modifies the apparent angle between the optical axis of the telescope and a point on the celestial sphere by an amount depending on the component of the spacecraft's velocity vector along the line of sight. During the course of an observing session the angle between the HST's velocity vector and its optical axis changes as the spacecraft orbits the Earth, thereby changing the apparent angle between the optical axis and a given point on the celestial sphere. It is possible to repoint the telescope continuously to maintain the angle between its optical axis and a single, chosen position on the celestial sphere, or equivalently, to keep the light from a patch of sky at given RA and Dec focused at a chosen *alignment point* in HST's focal plane. However, it is impossible to do so across the entire field of view of an FGS. Therefore, the measured position of an object within an FGS must be corrected for differential velocity aberration.

The factors that contribute to the overall error of this correction include uncertainties in the relative positions of the three FGSs, and hence the precise V2,V3 coordinates of the astrometry targets, plus uncertainties in the guide-star coordinates and the location of the alignment point. Other contributing factors include errors in HST's orbital ephemeris and the Earth's heliocentric ephemeris. Inspection of one-minute integrations of the (V2,V3) coordinates of the dominant guide star, corrected for this aberration, over the course of the visit provide a good assessment of the overall residuals to be expected from the differential velocity aberration correction. While these corrections can be as large as 30 mas (under suitable geometric conditions) the corrected dominant guide star positions repeat at sub-millisecond of arc. Therefore, the correction for differential velocity aberration is estimated to be uncertain at about ± 0.3 mas.

12.2.8 Lever Arm Length and Offset Angle

Early in the HST mission it became clear that FGS 3 was undergoing a scale change over time. Such changes were not unexpected because several of the optical elements in the instrument are mounted on graphite-epoxy composite surfaces known to absorb water vapor at atmospheric pressure and to outgas once in orbit, changing the alignments within the instrument and the effective scale of the detector space. Monitoring of the standard astrometric field M35 has helped to

track these changes, leading to time-dependence of Star Selector A's lever arm length and offset angle. These corrections are referred to as the *RhoA* and *KA* corrections.

Although there is little physical basis for the success of this approach, the result is the preservation of the internal relative scale and a minimization of temporally evolving gradients to the OFAD calibration. The uncertainties which remain after this correction are estimated from the residuals of plate comparisons of the individual visits in the calibration program. Over the entire field of view of FGS 3, the rms residuals are typically 2 mas along the *x*-axis, 3 mas along the *y*-axis. Much better performance is achieved in the central region of the pickle, 1mas on each axis.

12.3 Visit-Level POSITION Errors

A POSITION mode observing program uses the FGS to derive the relative angular separations of several objects distributed across an astrometric field. In traditional astrometry, images of objects are recorded simultaneously onto a photographic plate, and the plate is later analyzed to determine the relative separations of the objects. Astrometry with the FGS, by contrast, proceeds in the reverse order; the positions of the individual objects are found first, and then a virtual plate is constructed with the help of data from the guide stars and check stars.

Both approaches must deal with optical field angle distortions, lateral color shifts, and plate scales. However, FGS measurements are far more vulnerable to temporal variations that might occur during the observing sequence. The challenge is to assemble an astrometric plate by defining a common but arbitrary coordinate system onto which the individual observations are mapped. Observers must assume that the telescope's yaw, pitch, and roll might be slightly different for each observation, causing the sky to wobble about in FGS 3's detector space. Such motions can be detected and eliminated using guide star data and check star measurements. Corrections based on guide star data are referred to as *POSITION mode dejittering*, and those based on check star data are called *drift corrections*. Here we discuss the errors associated with each procedure.

12.3.1 POSITION Mode De-jittering Errors

During a nominal FGS visit, two FGSs guide the telescope, tracking their guide stars in FineLock, while the third sequentially measures the positions of the astrometry targets in detector space. As described in "Assembling the Visit" on page 11-5, the pointing control system uses one of the guide stars, called the dominant guide star, to minimize unintended translation of HST's optical axis across sky. It uses the other, called the roll star, to control the rotation of the focal plane. The section "POSITION Mode Pipeline" on page 11-3 describes how the POSITION mode pipeline accounts for spacecraft jitter during a visit by mapping

all observations into the frame defined by the guide star centroids during the first observation.

The adjustments to the astrometry centroids from this POSITION mode de jittering correction are typically about 1 mas. However, the corrections occasionally can be as large as 5 mas for one or two observation of a visit. These large corrections arise most frequently when orbital day-to-night or night-to-day transitions excite HST's vibrational modes. During such events the residuals depend upon the amplitudes of these excited modes but are estimated to be typically about 1 mas. During quiet times, the residual of this correction is about ± 0.3 mas.

12.3.2 Drift Correction Errors

As discussed on page 11-6, astrometry targets observed multiple times per visit typically drift across the FGS by about 6 to 12 mas when two FGSs guide the telescope and by up to 70 mas with only one FGS guiding. Because astrometry observations execute sequentially, the resulting errors in the measured angular separations between objects increase as the time between the measurements lengthens. The pipeline must then remove an effect that is typically 4 and not infrequently up to 25 times the overall astrometry error budget (2.7 mas).

To remove this drift, the calibration pipeline applies a model derived from the check star data to all the observations in the visit. The residuals from this correction are difficult to quantify in the usual way because the standard deviation of the data from a fit means little if only three to five points determine the fit. On the other hand, the success of the drift correction is clearly demonstrated by comparing the residuals of two plate overlays, one where the individual visits are drift corrected, the other not. Provided adequate check star data are available to generate a reliable model, plates with the drift correction applied correlate well, typically with 2 mas rms residuals. At minimum, two check stars should be observed three times each. Residuals between those same visits without drift correction range up to 15 mas rms.

Recall that the pipeline can generate three separate drift models: Linear, Quadratic, or Quadratic with rotation.

The first two models are translational only. The third model requires more than one check star and is unreliable if there are not enough visits to any given check star. The pipeline applies all three algorithms, where applicable, and computes chi squares and degrees of freedom for each result. The observer should review these data to determine which result is best suited for further data processing. Experience has shown that often one cannot determine which drift model is best until data from several visits are compared and the plate overlay residuals are evaluated.

12.4 Field-Level POSITION Errors

POSITION mode astrometry involves observations of several objects in a given visit followed by subsequent visits to the same field over the lifetime of the observing program, which can span years. The scientific goal is typically to measure systematic temporal changes in the angular separations between one or more objects and the reference field. Just as the individual observations in each visit must be mapped onto a common fixed coordinate system to define the visit's virtual plate, the visits themselves must also be mapped to a common reference frame to produce a *plate overlay* (see “Plate Overlays” on page 13-3). The errors associated with several of the pipeline corrections will not manifest themselves until data from individual visits are compared via the plate overlay process.

A plate overlay is performed by translating and rotating the individual plates from each visit and adjusting their relative scales to form a single master plate common to all visits. The locations of the individual reference stars on each plate determine how to map the data from that visit onto the common master plate. Because the reference star positions for each visit are themselves slightly uncertain, the master plate will not be error free but rather an optimal compromise. The quality of the fit for a given visit can be assessed by comparing the positions of the reference stars in that visit with their positions on the master plate. The rms residuals of the fit, referred to as the *plate overlay residuals*, can be as small as 1 mas or as large as 6 mas.

Two commonly used plate solutions are the four-parameter and the six-parameter plate solutions (see Chapter 13). The four-parameter solution adjusts for translation, rotation, and relative scale, while the six-parameter solution adjusts the relative scale independently along the x and y axes. The six-parameter solution can be used only when enough reference stars are available to provide the necessary degrees of freedom. Typically five or six reference stars will suffice; otherwise, the four parameter technique must be used.

Often an observer realizes that the reference stars, initially assumed to be fixed on the sky, in fact do have measurable parallaxes and proper motions. If these apparent motions are not accounted for, they will contaminate the master plate, resulting in needlessly large residuals that compromise the scientific investigation. For the sake of overall error assessment, let us assume that all the stars in every visit are fixed on the sky, so that any residuals in the master plate can be traced to errors in the individual measurements made during the individual observations.

The most dominant source of error in POSITION mode data reduction is the OFAD correction, followed by the uncertainty of the corrections to the star selector RhoA and KA values used in the pipeline for a given epoch. The third most important source of error is the drift correction. The size of this error depends most importantly upon the check star scenario used and to a much lesser extent the amplitude and temporal signature of the drift experienced during the visits.

Target magnitude is not an important contributor to the overall error until $V > 16$, after which it quickly can dominate. Before the DIFF/SUM correction

was added to the pipeline, stars with $V > 15$ were found to have large residuals in the plate overlays (> 4 mas). With the DIFF/SUM correction, such residuals have decreased to about 2.5 mas.

The cross filter effect (F5ND to F583W) contributes only about 1 mas to the residual of targets requiring this correction, provided the observations are made at a place in the FGS where this effect has been calibrated. The lateral color effect, not corrected for in the pipeline, shows up either as noise or is absorbed in a correction for presumed apparent parallax of a reference star.

Table 12.3 summarizes the contributions from a variety of sources to the overall POSITION mode error budget. Also indicated are the typical size of the corrections that are made during the calibration process. If these errors were “root sum squared,” the resulting uncertainty would be about 2.7 mas (for bright stars). Note that these estimates are based on a number of assumptions about the observation strategy and star distribution across the pickle: it is assumed that all of the stars are brighter than about $V = 14.4$, that they are widely distributed across the pickle, and that an adequate check star scenario was used in the observing sequence.

Overall, the plate residuals for a field of numerous bright stars confined to near the pickle's center can be as small as 1 mas per axis. More often the observer finds that the reference field is sparse or faint, the stars are not confined to the central region of the FGS, or that an optimal check star strategy was not used. In less optimal cases with these deficiencies, the residuals might still be as good as 3 mas but can be as dismal as 7 mas.

Table 12.3: POSITION Mode Corrections and Errors

Correction	Size (mas)	Error (mas)
Median of FL data	–	~1, $V < 14.5$ ~3, $V > 16$
Diff/Sum	1–5	~1
LTSTAB	> 100	~1.5
OFAD	> 4000	~2.2
Diff. Vel. Aber.	0–30	< 0.5
HST jitter	0–5	< 0.5
FGS drift	2–70	< 1
<i>Cumulative</i>	> 4000	~2.5 (on average)

12.5 TRANSFER Mode Errors

Automatic pipeline processing of TRANSFER mode data is limited to locating each scan in the astrometer's data file, editing out bad data arising from garbled

telemetry, and determining for each scan the median position and standard deviations of the guide stars. These activities do not introduce errors or uncertainties.

Chapter 13 describes the techniques and procedures used to derive angular separations and magnitude differences of the components of multi-star systems or the angular sizes of extended objects. We will discuss the uncertainties associated with these analyses along with the procedures themselves.

We currently plan to upgrade the astrometry TRANSFER mode pipeline to perform more of the activities now carried out by the non-pipeline processing. As these upgrades come online, we will provide updated versions of this chapter via STScI's FGS WWW pages.

FGS Data Analysis

In This Chapter...

Analyzing Individual Observations / 13-1
Plate Overlays / 13-3
Resolving Structure with TRANSFER Mode / 13-5

Observers can analyze FGS astrometry data at various levels. Individual observations can be of interest when a particular star shows large, unexpected residuals. More frequently observers will be constructing plate overlays from sets of POSITION mode observations to determine parallaxes, proper motions, and reflex motions. Alternatively, analysis of TRANSFER mode observations can reveal an object's spatial structure at milliarcsecond scales. This chapter discusses the tools that will soon become publicly available to support these diverse astrometric investigations with the FGS.

Unlike the case for HST's other science instruments, STSDAS/IRAF does not currently provide tools supporting FGS astrometry. However, extensive and sophisticated software for analyzing both POSITION mode and TRANSFER mode datasets does reside at STScI. Most of this software was provided to STScI by the Space Telescope Astrometry Science Team (STAT) at the University of Texas and Lowell Observatory. Efforts are underway at STScI to make these tools available through the IRAF/STSDAS environment. Check the STScI FGS web pages for updates.

13.1 Analyzing Individual Observations

Sometimes an FGS observer may find that a single observation requires a detailed investigation, such as a particular star in a POSITION mode observation that appears on one or more plate overlays with large, unexplained residuals. The object might not be a single star as originally assumed, or perhaps a stellar flare occurred while the target was being tracked in FineLock. Either of these cases might become readily apparent through close inspection of the FineLock vs. Coarse Track centroids in the first case or the photometry data in the second case.

The interactive graphics tool **fgs_plotter** can display a variety of FGS quantities as functions of other data. For example, you can display the location of the IFOV in pickle coordinates as a function of x vs. y , or the fine error signal (partial S-curve) as a function of x during the WalkDown to FineLock. This tool works with guide star data as well as astrometry data.

The **fgs_plotter** tool is both versatile and essential for analyzing failed observations and retrieving useful data from marginal observations. For example, Figure 13.1, generated with **fgs_plotter**, shows a failed observation in which the FGS was not able to acquire a star in FineLock because the fine error signal (S_x) did not exceed the necessary threshold. The tool can also be a valuable educational aid for an observer who is unfamiliar with FGS data. Figure 13.2 shows the menu of functions in FGS_PLOTTER that are available to the observer.

Figure 13.1: Example of a Failed Observation Analyzed with FGS_PLOTTER

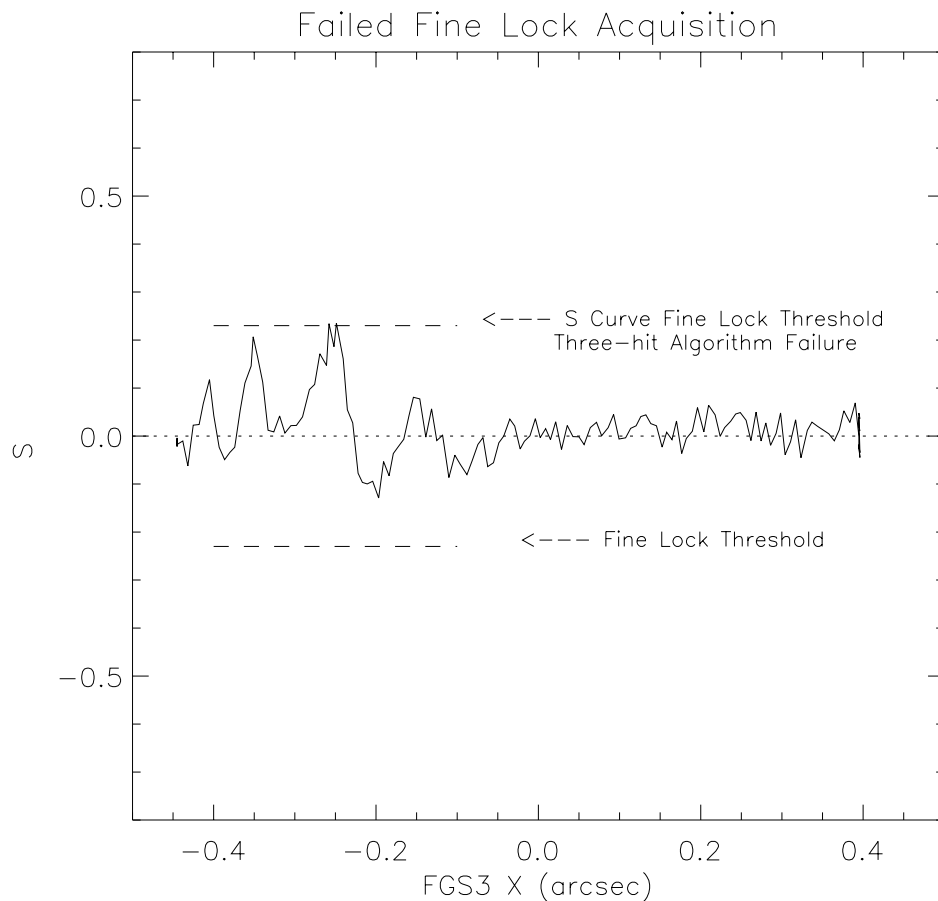


Figure 13.2: Options Available in FGS_PLOTTER

```

NAXIS1 = 108520

Table of graphics options:
Select the desired graphics option

(1) X vs. Y
(2) Sx-curve vs. x-axis      (A) X          (H) PMTYA
(3) Sy-curve vs. y-axis     (B) Y          (I) PMTYB
(4) Rx vs. X                (C) Sx-curve  (J) [PMTXA + PMTXB]
(5) Ry vs. Y                (D) Sy-curve  (K) [PMTYA + PMTYB]
(6) x-position vs. time     (E) Time      (L) PMTsum
(7) y-position vs. time     (F) PMTXA     (M) Theta A
(8) Sx vs. time             (G) PMTXB     (N) Theta B
(9) Sy vs. time
(10) [PMTXA + PMTXB] vs. time
(11) [PMTYA + PMTYB] vs. time      (Z) I/O Parameters
(12) PMTsum vs. time
(ZX) co-added X s-curves          (UX) FESAVG_X
(ZY) co_added Y s-curves          (UY) FESAVG_Y
(XA) co_added XA pmt counts       (XB) co_added XB pmt counts
(YA) co_added YA pmt counts       (YB) co_added YB pmt counts
(XS) co_added XA,B pmt counts     (YS) co_added YA,B pmt counts

Your choice (^Z for help) ->

```

13.2 Plate Overlays

Plate reductions are necessary to measure the parallax, proper motion, and reflex motion of a given object with respect to the reference field star. To generate a plate overlay, calibrated pipeline data from several visits—possibly spanning years—are collected and mapped onto a common reference frame, or *virtual plate*. It can then be determined whether the object of interest moves in a systematic, time-dependent way with respect to the reference field. The Space Telescope Astrometry Science Team (STAT) has developed a very useful tool for constructing plate overlays and has made it available to STScI for development into a publically accessible tool.

The plate overlay tool derives a virtual plate using either a four parameter or six parameter plate solution. The four parameter model adjusts for translation, rotation, and relative scale, while the six parameter model adjusts the relative scales along the x and y axis independently. Formally the six parameter model requires at least three common reference stars in each plate, but in order to avoid over-constraining the plate solution, you should not apply the six parameter model with fewer than five reference stars.

Ideally the object under scientific investigation should not enter into the virtual-plate solution. Only the mapping functions should be applied to the object, so that any apparent motion of the object with respect to the reference frame will not be identified simply as a large residual. Unfortunately, some observers may find it necessary to include the science target in the solution if in fact one or more of the reference stars must be disqualified, as would be necessary if the reference star were a binary.

Applying the six parameter model to a plate with fewer than five reference stars might over constrain the solution, making it vulnerable to contamination from unknown and unaccounted for proper motion or parallax in one or more of

the reference stars. Such motion would be absorbed undesirably into the solution. Clearly, if the mapping of the individual plates onto the virtual plate is flawed in any way, the scientific objectives will be compromised.

When the six parameter solution is suitably constrained, it noticeably enhances the overall quality of the plate overlays. Indeed, the known tendency of HST's magnification to oscillate or "breathe" by small amounts during an orbit alters FGS3's plate scale by different amounts in the x and y directions. The same effect occurs on longer time scales, owing to the continual desorption of the optical telescope assembly and consequent refocusing every several months. Therefore the focus of HST varies with time, resulting in different relative scales along the x and y axes among a set of astrometric visits. A six-parameter model is most appropriate in such situations, but again, it can be risky if fewer than five reference stars are available.

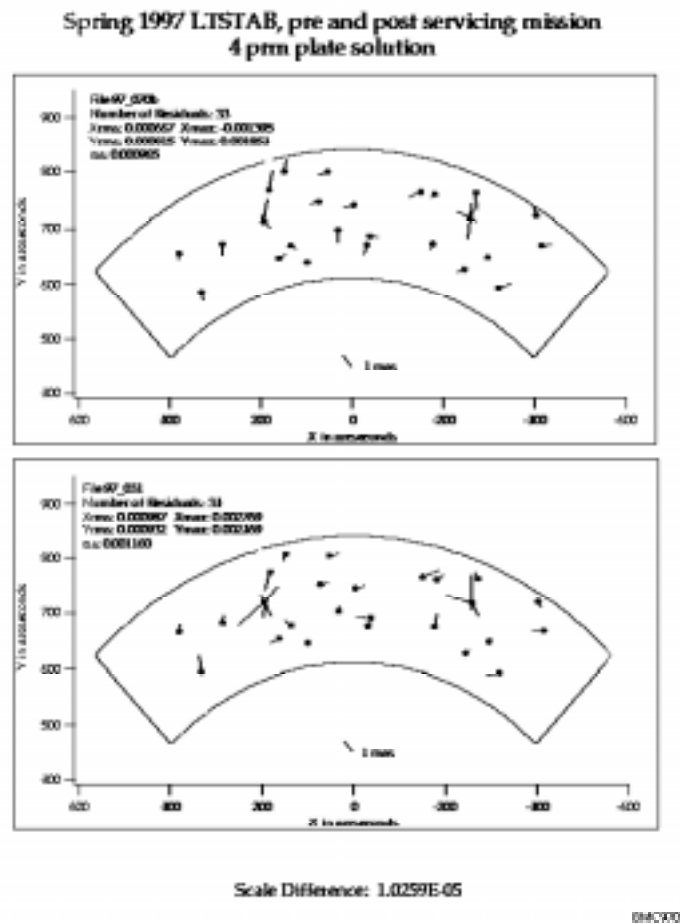
The four-parameter model has so far been the workhorse for obtaining FGS astrometric plate solutions because the reference fields around the scientific targets have frequently been too sparse for a six-parameter model. Formally only two reference stars are needed to apply the four-parameter model, but obviously such a solution is highly constrained and vulnerable to motions of the reference stars and errors in their measured positions.

It is not uncommon for an observer to delete at least one reference star from the plate solution for a variety of reasons. For example, the star could be double, fooling the FGS into locking onto one component on the x -axis and the other on the y -axis during one visit, then some other combination on subsequent visits. Or, the star might be significantly fainter than anticipated, preventing the FGS from reliably acquiring it in FineLock.

Another frequently encountered problem with the plate solutions is for one or more of the reference stars to display an unanticipated but detectable proper motion or parallax. If the star field is observed frequently enough over a sufficiently long period of time, at various HST roll angles to optimize sensitivity to proper motion, then these motions can usually be determined with acceptable accuracy. If so, the measured position of such an object at a given epoch can be adjusted for its apparent motion before the data from that visit are mapped onto the master plate. Unfortunately, corrections of this nature are usually only possible if the observer has the luxury of an adequate number of otherwise well behaved reference stars. Figure 13.3 shows the residuals from a four-parameter plate solution for two visits to a standard astrometric field. The agreement is all the more impressive in this case because HST rolled by more than 25 mas in one of the visits during the observing sequence.

When the plate overlay software becomes publicly available, it will be announced and documented on the STScI web pages.

Figure 13.3: Residuals of Two Virtual Plates Overlaid with a Four-Parameter Plate Solution



13.3 Resolving Structure with TRANSFER Mode

TRANSFER mode observations with the FGS can resolve the individual components of multiple star systems and measure the angular diameters of extended objects. These observations scan the instantaneous field of view (IFOV) of the FGS across an object to accumulate the necessary data for a post observation reconstruction of the x and y axis S-curves. The GO compares the observed S-curves to those from a reference star in the calibration database to deconvolve the contribution from each component of a multi-star system or each chord of an extended object. Such an analysis can reveal the magnitude difference and relative separation of a binary star system or the apparent angular diameter of an extended object in both the x and y directions.

Routine pipeline processing of TRANSFER mode data, discussed in Chapter 11 is confined to locating the individual scans within the data files,

editing out bad data, and computing guide star centroids and standard deviations during each scan. Otherwise TRANSFER mode observations have always been processed interactively rather than through a pipeline, which is why we discuss them here as a form of FGS data analysis. In the near future the pipeline will be upgraded to perform extensive data reductions on TRANSFER mode observations (see Chapter 11) in order to support the mixed-mode approach, which combines TRANSFER mode observations with POSITION mode observations made in the same visit. More specifically, the pipeline modifications will enable the results from TRANSFER mode observations to be used along with the POSITION mode observations in the construction of virtual plates. The ultimate goal is to support the scientific determination of parallaxes, proper motions, and reflex motions due to dark companions of multi-star systems resolvable with the FGS.

13.3.1 FGS Response to a Binary

In their purest form, TRANSFER mode observations are made to resolve a close binary pair, to monitor it over time, and to derive its orbit. Unlike radial velocity studies, an orbit determined by the FGS reveals the system's inclination. Additional information about the system's parallax or radial velocities can be used to determine its masses. In order to clarify how TRANSFER mode observations determine binary separations and relative intensities, we will first discuss the response of the Koester prisms to the wavefront from a binary star.

The wavefront of a point source at the face of a Koester prism is collimated, coherent, polarized, and characterized by a propagation vector. As the instantaneous field of view of the FGS scans across the target, the tilt of the wavefront varies and the PMTs register different relative intensities. Plotting the position of the IFOV along the scan path against the normalized difference of the PMTs thus reveals the characteristic S-curve of the FGS (see "S-curves" on page 9-8).

If the source is a double star, then its wavefront at the face of the Koester prism will have two components, each coherent with itself but incoherent with respect to the other. Two propagation vectors characterize this wavefront and the angle between them is directly related to the angular separation of the stars on the sky. As the FGS's IFOV scans across the object, each component of the wavefront generates its own S-curve, whose modulation is diminished by the non-interfering background contribution from the other component. The interferometric null for each star occurs at a different point along the scan path, so the resulting relationship between the position of the IFOV along the scan path to the normalized difference of the PMTs depends upon both the separation of the stars and their relative brightnesses. To demonstrate this effect, Figure 13.4 shows the FGS 3 y-axis S-curves of several synthetic binary systems with a variety of angular separations and relative intensities.

Figure 13.4: Effect of Double Stars on S-curve

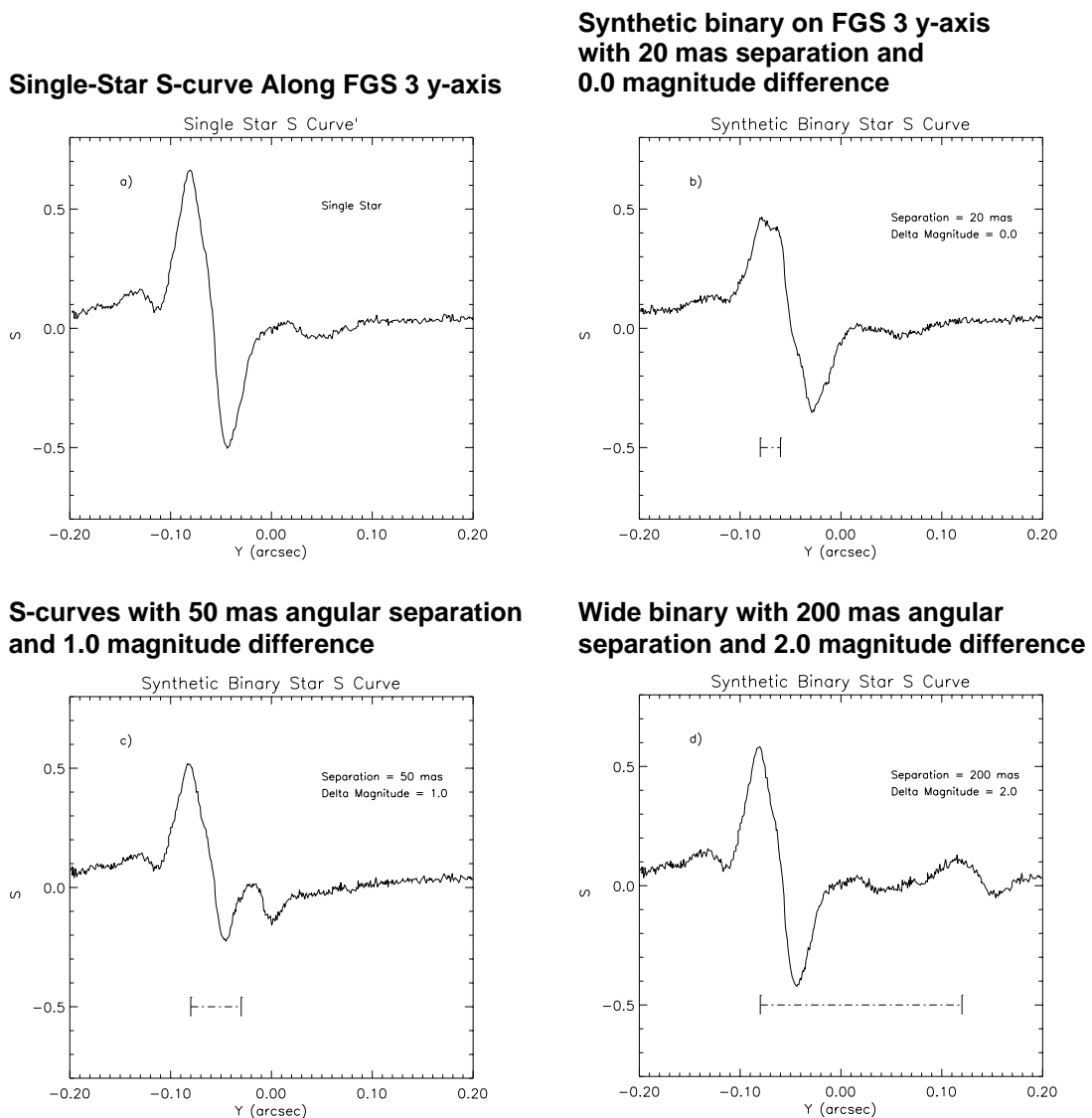
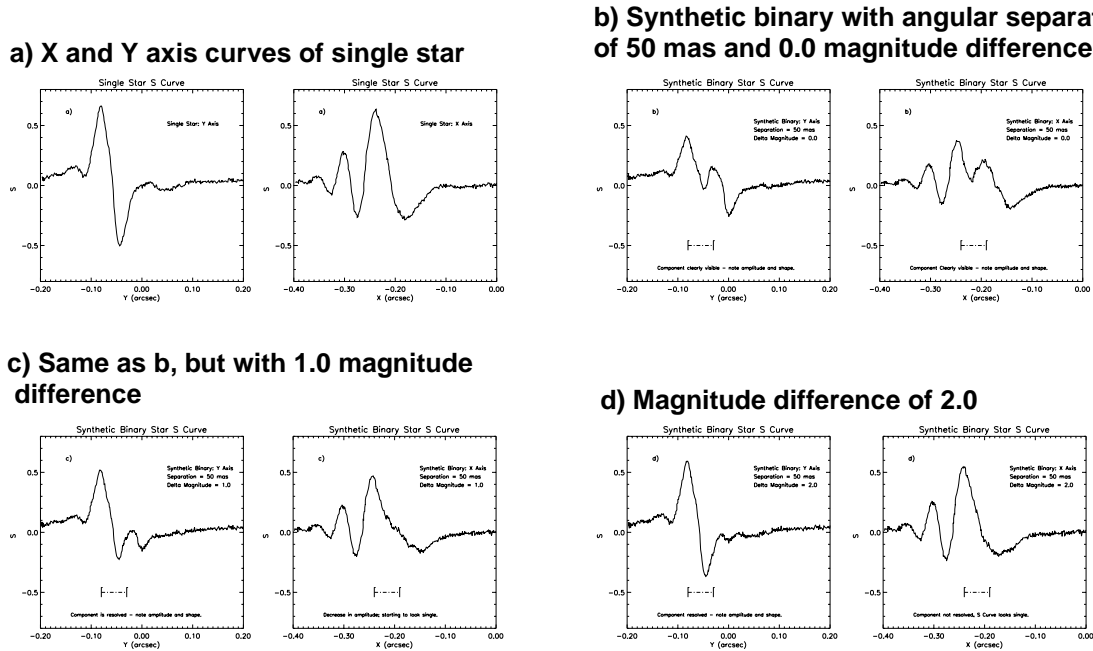


Figure 13.5: Resolving Power of FGS 3 Dependency on Characteristics of Single Star S-curves. Note that the x-axis S-curve in (d) "looks" more like the single star s-curve in (a) than does its cousin along the y-axis, demonstrating the enhanced resolving power along the y-axis relative to that along the x-axis.



If the angular separation of the stars is greater than the characteristic width of an S-curve, two distinct S-curves will be apparent, but the modulation of each will be diminished relative to that of a single star by an amount depending on the relative intensity of each star. On the other hand, if the angular separation is sufficiently small, the S-curves will be superimposed, and the morphology of the resulting blend will be complicated. In either case, the composite S-curve can be deconvolved using reference S-curves from point sources, provided the angular separations are not too small and the magnitude difference is not too large. To be more precise, fitting the observed double star S-curve with two appropriately weighted, linearly superimposed reference S-curves from single stars can determine the angular separation and magnitude difference of the binary's components.

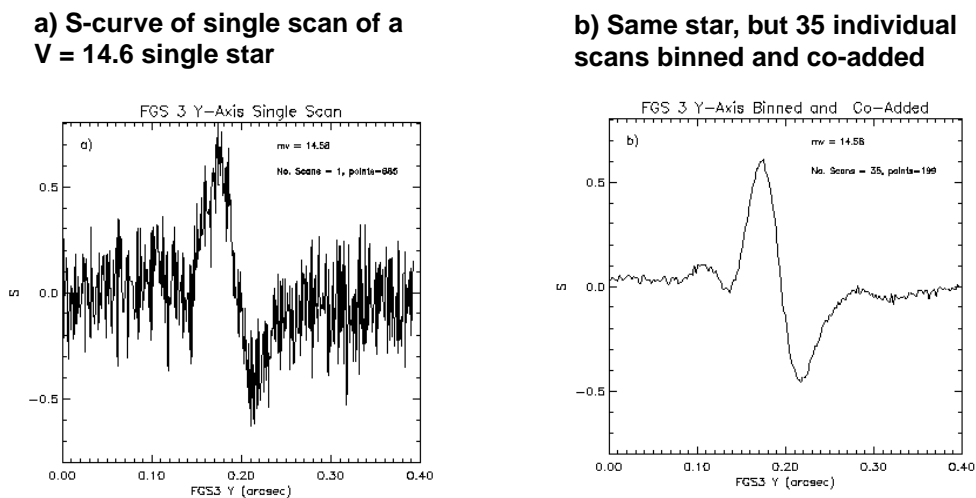
The modulation and morphology of its point-source S-curves ultimately determines the resolving power of the FGS. Figure 13.5 diagrammatically demonstrates how the amplitude of the S-curve couples with the magnitude difference of the binary to determine the FGS's resolving power. It shows a synthetic binary star system with an angular separation of 50 mas on both the x and y axes of FGS 3, but at a variety of relative intensities. It is clear that as the magnitude difference increases, the resolving power of the FGSs along the x -axis becomes doubtful well before that of the y -axis. Note, however, that this separation and selection of magnitude differences was chosen solely for its visual impact. The data reduction algorithm would have no difficulty resolving the binary in Figure 13.5c.

13.3.2 TRANSFER Mode Data Reduction

After the astrometry pipeline locates and extracts the individual scans of a TRANSFER mode observation, the resulting data files are ready for further analysis. Currently, the steps involved in routine TRANSFER mode data reduction are:

1. Visual inspection of the S-curves from each scan to identify and disqualify those corrupted by vehicular jitter or data dropouts.
2. Dejittering of the astrometry data at 40 Hz using the instantaneous position of the dominant guide star in its FGS, if desired. (This step may requalify scans that would otherwise be deleted from further consideration.)
3. Cross-correlation of each scan, in order to detect any drift of the FGS across the sky during the course of the observation.
4. Shifting of each scan by the amount determined necessary in step (3) so that all scans are mapped to a common reference frame.
5. Binning and co-adding of the individual scans to generate a high signal to noise composite S-curve. Each step of the IFOV along each scan is placed into an appropriate bin, and then all entries in a given bin are averaged to produce the high S/N binned and co-added S-curve. See Figure 13.6.
6. Fitting of a piecewise third order polynomial fit to the binned and co-added S-curve.

Figure 13.6: Benefits of Binning and Co-adding of Individual Scans



If the observation is a calibration measurement, the goal of the calibration proposal will drive the subsequent analysis of the data by the FGS group at STScI. For example, if the object was observed to obtain a color calibration of a single star, the data will be inspected to assure that the object does in fact appear to be single star. If so, the raw and processed data will be entered into the FGS calibration database and be made available to the observer.

If the observation under analysis is of a binary star system and the observer wishes to determine the angular separation and magnitude difference of its components, the following additional tasks are undertaken.

7. Selection of an appropriate set of reference S-curves from the calibration library on the basis of the target color (or colors) and the dates of observation of both the binary system and the calibration stars. These dates should be as close as possible to minimize the impact of temporal variations in FGS3.
8. Fitting the binary system's composite S-curves with the reference S-curves by iteratively determining the angular separation and magnitude difference. This fitting is done on both the x and y axis. The quality of the fit can be assessed by comparing the magnitude differences determined independently along each axis.

On the other hand, if the observed target is an extended object, the GO will retrieve the appropriate reference S-curves from the calibration data base and use software tools appropriate for such an investigation.

Whether the observation be of a calibration star, a binary system, or an extended source, STScI will be producing publically available software packages to support the analysis of these data. Please consult the STScI FGS Web pages for updates.

13.3.3 Uncertainties in TRANSFER Mode Data

This section discusses several error sources associated with analysis of TRANSFER mode data:

- Spacecraft jitter.
- FGS drift.
- Temporal variability of the S-curves.
- Wavelength dependence of the S-curves.
- Roll dependence of the FGS plate scale.

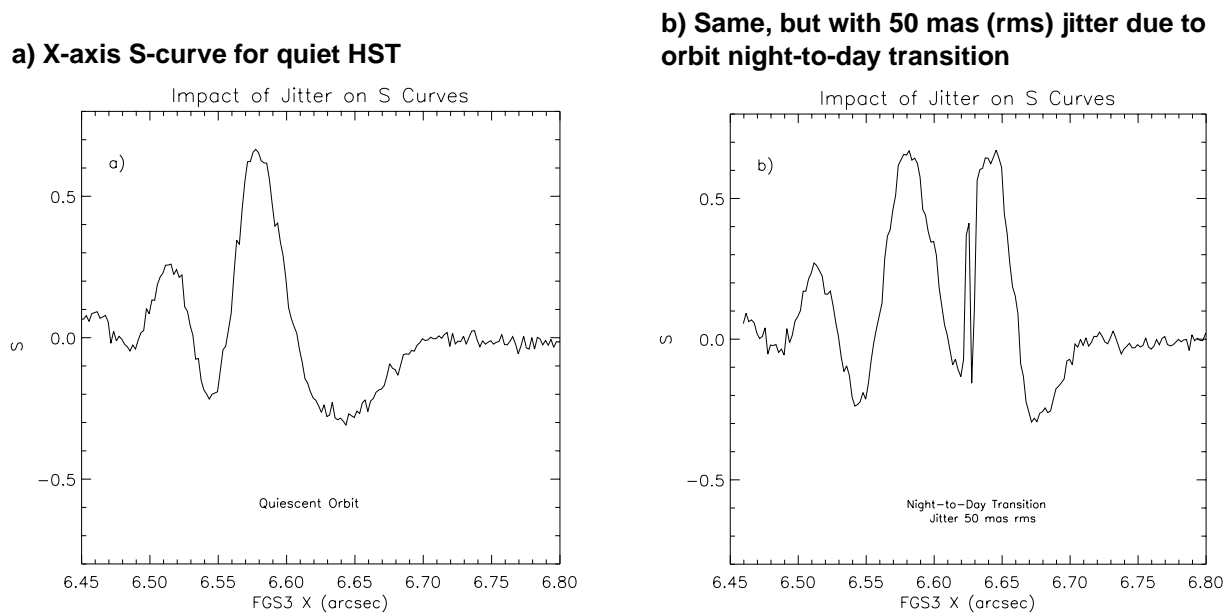
Spacecraft Jitter

When the FGS is used as an astrometer in TRANSFER mode the observer specifies several individual scans of the target in a particular visit, typically between 15 and 35. Periods of extreme spacecraft jitter or telemetry dropouts can compromise the data from an individual scan. Mild jitter of the spacecraft, at the level of 20 mas peak-to-peak, is repairable by using the guide star data to remove the apparent wobble of the sky in the astrometer's aperture. In the most extreme cases, it may be necessary to disqualify a number of scans from further analysis.

To obtain high signal-to-noise S-curves, the single scans must be cross-correlated, shifted, binned, and co-added. Any small, unaccounted for spacecraft motion that occurs during each scan will effectively blur the boundaries of the binning procedure, ultimately causing the co-added S-curve to suffer some loss of spatial resolution. This effect invariably occurs because even a 40 Hz

de-jittering of an astrometry observation executed during the quietest of HST orbits will not escape the residual jitter introduced into the pointing control system by the guide stars' photometric noise. Thus, the maximum resolving power of an FGS in TRANSFER mode can not be better than about 1 mas. Figure 13.7 compares the S-curves from two single scans, one obtained during a nominally quiet HST pointing, and the other observed during a time of high spacecraft jitter.

Figure 13.7: Comparison of S-curves from Two Separate Scans during Same Observation



FGS Drift

As discussed in the calibration chapter, astrometry stars observed in POSITION mode more than once in a given visit reveal that the FGS's total field of view drifts across the sky over the course of an HST orbit. This drift is also apparent in TRANSFER mode observations. The cross-correlation of S-curves prior to binning and co-adding automatically accounts for drift in TRANSFER mode observations. Each single-scan S-curve is shifted so that the particular feature of the S-curve used for the cross correlation coincides with that of the fiducial S-curve. The reliability of implicitly removing the drift is only as good as the accuracy of the cross correlation procedure.

Proper cross correlation is relatively straightforward for bright objects ($V < 13$), but for fainter objects it becomes more difficult, just as binning and co-adding becomes all the more important. In such cases it might be advantageous to construct a drift model iteratively by time tagging the shifts determined by the cross-correlation procedure. Fitting of these shifts to a linear or quadratic drift model might align the individual S-curves more reliably than a procedure that depends solely on individual noisy scans. For bright stars with $V < 13$, drift in the FGS is estimated to degrade the resolution of TRANSFER mode observations by

about 1 mas. For fainter stars, the degradation will increase significantly in a way that depends on details of HST's orbital environment during the visit. Recall from the discussion of drift on page 12-12 that its origin is not well understood. It is not repeatable, and its amplitude depends weakly upon the declination of HST's V1 axis. If a particular observation of a faint star ($V > 15$) was subject to typical drift of around 10 to 12 mas, then the estimated loss of angular resolution would be about 4 mas.

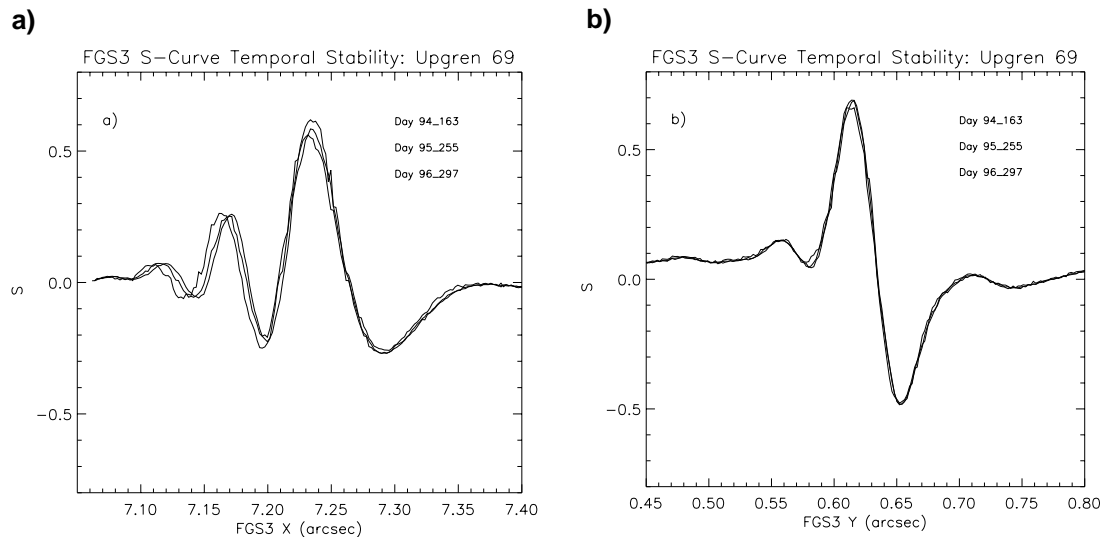
Temporal Variability of S-Curves

Measurements of the standard star Upgren69 over the lifetime of FGS3 have indicated 1–2% temporal variability of the shapes and the peak-to-peak amplitude of its S-curves. The magnitudes of these changes can have important consequences in the reduction of binary star data when the separation of the components is less than 20 mas and the magnitude difference exceeds 0.6. These temporal changes also affect analyses of extended source observations. There are three ways to minimize the effects of temporal S-curve instability:

- Obtain reference standard star data at the time of the observation. (S-curves appear to remain stable over at least a few months.)
- Select from a library of calibration S-curves taken over the course of the cycle the one closest in time to the target observation.
- Determine a correction algorithm which interpolates in time between S-curves taken from the S-curve library.

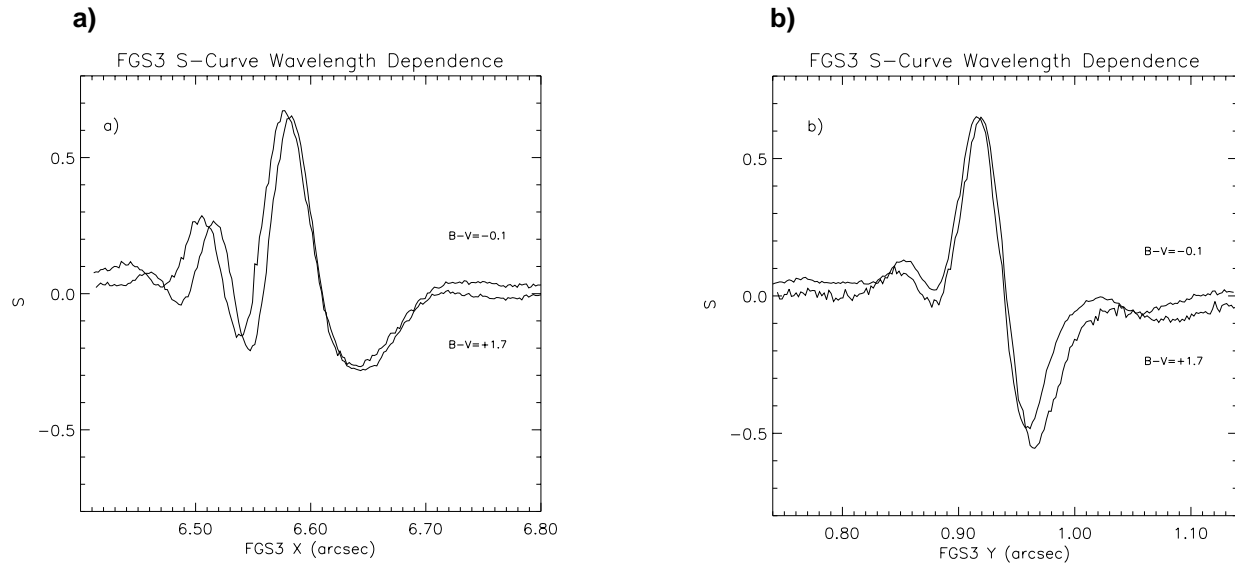
Calibration standards for multiple component systems with small separations and large magnitude differences may have to be observed in the same epoch as the target as part of the proposed observing program. For less constrained programs, selection of reference S-curves close in time to the observation should be adequate. The STScI Cycle 7 calibration program contains a monitoring program which will allow us to establish the size of the S-curve variability and to assess its time scale coarsely. We will determine whether or not we can derive a correction algorithm as these data accumulate. Figure 13.8 shows the variability of FGS 3's S-curves over a time period exceeding two years.

Figure 13.8: Temporal Changes in FGS3's x and y axis S-curves from 6/94 to 9/95 to 10/96). Notice the larger changes along the x-axis while the y-axis remains quite stable.



Wavelength Dependence of S-Curves

S-curves are also wavelength dependent. Semi-empirical modeling has shown that when the difference between a standard reference star color and the target star color, $\Delta(B-V)$, exceeds 0.2–0.3 magnitudes, the residuals of the deconvolution begin to degrade the reliability of the binary star analysis. To deconvolve a binary system, reference scans of the appropriate colors, scaled by the relative brightnesses, are required. Models and extrapolations have yet to reproduce this wavelength dependence of the FGS S-curves with acceptable accuracies. The optical train is very complex, and the database of reference transfer functions to date is not comprehensive. The current STScI calibration program includes observations of single reference stars whose colors are comparable, within 0.2–0.3 magnitudes, to the targets in the GO programs. These are observed about once per cycle and are available in the standard reference library. As we build up this color library, we will investigate further these effects, and the possibilities for improved modeling, with the objective of providing observers the means to generate a single-star reference S-curve for exactly the color required. Figure 13.9 shows how the S-curves in FGS3 respond to the color of the object. Note that both the x and y S-curves respond to the color effect, unlike the temporal changes which affect mostly the x -axis.

Figure 13.9: Effects of Star Color on FGS S-curves

TRANSFER Mode Plate Scale and HST Roll

Several observing programs have revealed that the measured separation of a binary system is sensitive to its orientation relative to the FGS interferometer axis. The impact of this dependence on the HST roll angle is to introduce systematic variations into the binary's orbit. In some cases, these variations could masquerade as perturbations by massive dark companions. Hughes Danbury Optical Systems has developed a model for this effect, which involves a linear relation between the separation of the components derived from the S-curves and the roll at which the data were obtained. The error is a few percent ($< 3\%$) of the separation, scaling linearly with separation, so binaries with large separations (> 200 mas) are affected more than those with small angular separations.

This effect is believed to be due to a rotation of the Koester prism about the normal to its entrance face. The Cycle 7 calibration program incorporates a test that will be used to verify and fine-tune this model, and the results will be made generally available as an STSDAS calibration tool. Check the STScI FGS WWW pages for updates.